MODELING OF POLYAMIC ACID AND POLYIMIDE REACTORS

A Thesis Submitted

in Partial Fulfilment of the Requirements

for the Degree of

MASTER OF TECHNOLOGY

by

SURENDRA KUMAR VERMA

to the

DEPARTMENT OF CHEMICAL ENGINEERING

INDIAN INSTITUTE OF TECHNOLOGY, KANPUR

APRIL, 1996

CHE—1996—m—VER—

121492

CERTIFICATE

This is to certify that the work contained in this thesis, entitled **Modeling of Polyamic acid and Polyimide Reactors** has been carried out by **Surendra kumar Verma** under my supervision and this work has not been submitted elsewhere for a degree.

April, 1996

Dr. Santosh K. Gupta

Professor

Department of Chemical Engineering

Indian Institute of Technology

Kanpur, INDIA

CONTENTS

ACKNOWLEDGEMENT

I wish to express my gratitude to my thesis advisor Prof. Santosh K. Gupta for providing me *constant* encouragement and motivation *all* the time during the reasearch work. I feel myself privileged to work under his guidance. It is from him I learnt what the systematic approach is.

I would like to thank Prof. Anil Kumar and Prof. S. K. Dogra for their critical views on this work.

I would like to thank my labmates Kohli, Chakravarty, Bhargav, Sajith, Mankar, Kislay and Pallav. Thanks are due on my classmates Raman, Gandhi, Upadhaye, Kansal, Rathi and Ritivik who made my stay here a memorable one.

<div align="right">Surendra Kumar Verma</div>

Rxns. 1, 3; Curve h: Rxns. 1, 2.

LIST OF TABLES

NOMENCLATURE

$-A$	Anhydride end group
$-A'$	Diacid end group
$-AB-$	Favoured conformer of amide link
$-A^{*}B-$	Imide link
$-A^{\#}B-$	Unfavoured conformer of amide link
A_i	Frequency factor
$-B$	Amine end group
$-COOH$	Acid group
E	Objective function
E_i	Activation energy for i^{th} reaction
f_{AB}	Fraction of favoured conformer of amide link
$f_{A^{*}B}$	Fraction of imide link
$f_{A^{\#}B}$	Fraction of unfavoured conformer of amide link
$-I$	Sum of favoured, unfavoured conformer of amide links and imide link
k_i	Forward rate constant of ith reaction
k_i'	Reverse rate constant of ith reaction
M_n	Number average molecular weight
M_w	Weight average molecular weight
PDI	Polydispersity index
P_n	Polymeric species of chain length n
$\underset{\sim}{\mathbf{p}}$	Vector of parameters
R	Universal gas constant (J mol^{-1} K^{-1})
t	Time (s)
t_f	Total reaction time (s)
T	Temperature (^{O}C or K)

w_i Weightage factor for i^{th} data point

W   Water

Greek Letters

λ_j^k k^{th} moment of jth species as given in Table 3

$(k = 0, 1, 2, \ldots)$;

$$\lambda_i^k = \sum_{n=1}^{\infty} n^k [P_{n,j}] \quad (mol\ m^{-3})$$

Subscripts / Superscripts

expt   Experimental values

f   Final values

0   Initial values

ref   Reference values

theor   Theoretical values

Symbols

[ ]   Concentrations $(mol\ m^{-3})$

ABSTRACT

A comprehensive kinetic model is presented which accounts for the major and side reactions present in polyamic acid and polyimide reactors. The mathematical framework is quite general, and permits incorporation of heat and mass transfer aspects typically encountered in large scale reactors. A few rate constants have been curve-fitted using some (limited) experimental data available in the open literature. Using these (and the other rate constants from the literature), some interesting phenomena have been predicted at higher temperatures. Detailed experimental data are required to evaluated all the rate constants with precision.

CHAPTER 1

INTRODUCTION

Polyimides are an important class of speciality polymers, exhibiting several desirable thermal and mechanical properties[1-4]. These include excellent electrical insulating capability and unusually high thermo-oxidative stability. Polyimides can be prepared by a number of reaction routes[3-6]. The most common among these is by the reaction between tetrabasic acid dianhydrides (e.g., pyromellitic dianhydride) with diamines (e.g., oxydianiline) in a two step process. In the first step, the two monomers react with each other in a suitable solvent [e.g., dimethylformamide (DMF)] at about $25^{\circ}C$ to give polyamic acid (PAA) precursors. Films or moldings of PAA are then cured at relatively higher temperatures of about $120-130^{\circ}C$. During this second stage, the PAA is converted to the polyimide by the dehydrocyclization reaction, while simultaneously releasing water as a byproduct. Since polyimides are relatively nonporous materials[7], this could lead to several technological problems like diffusional limitations (at a 'micro' level) of the reaction rate, crack and void formation, etc. The rate of volatile formation by chemical reaction must be synchronized with its rate of removal by mass transfer (at the 'macro' level), so as to minimize these problems. In addition, the water formed hydrolyzes the PAA molecules present and lowers the average molecular weight of the product. The properties of the polyimide product are, thus, affected by the average molecular weight of the PAA precursor, as well as the rate of the hydrolysis (and other) reactions. A proper design of these

reactors requires an understanding and modeling of the various physico-chemical phenomena associated with both these steps of polyimide manufacture. This study is an attempt along this direction.

An improved methodology of studying this system is discussed here, which is based almost totally on the kinetic approach. A kinetic scheme is presented (see Table 1), which incorporates the major reactions, as well as the important side reactions taking place in both the steps of polyimide manufacture. Mass balance and moment equations are written and appropriate moment-closure conditions[8,9] are developed. These equations are solved for an isothermal, well mixed batch reactor (first stage reactor in which the precursor is formed primarily). The Box[10] complex technique is then used to 'tune' those rate constants to which model results are most sensitive. This is done to minimize the sum of square of errors between the model predictions and experimental results of Kolegov et al.[11] for PAA synthesis.

The kinetic model developed herein provides a *general* mathematical framework for *both* the first and second (polyimide formation) stages of reaction, even though the model is tuned using data for the first stage only. *Qualitative* trends for the second stage (in absence of mass transfer limitations) have been predicted to illustrate the general nature of the model and its applicability at higher temperatures. Additional tuning of the other parameters against data may need to be performed once experimental results for the second stage become available in the open literature.

It should be added that this kinetic model can easily be

extended to predict some very interesting experimental observations described (qualitatively) by Johnson[7] such as the dependence of the average chain length of the product on the way in which the two *solid* monomers and the solvent are mixed in the reactor [e.g., higher molecular weight products are formed when the two solid monomers are blended in stoichiometric proportions and then added to a tank of pure solvent, than when either monomer (solid) is added slowly to a solution of the other monomer in solvent, etc.]. Such operations (involving mass transfer limitations) cannot be as easily modeled using the currently available theories[12-14], which involve varying amounts of probabilistic concepts.

CHAPTER 2

FORMULATION

The thermodynamics and kinetics of polyimide preparation have been extensively studied.[7,11,15-21] Table 1 gives the kinetic scheme incorporating most of the important reactions occurring during polymerization. This scheme is more general than that used by Kolegov et al.[11] (who omit the reactions asssociated with rate constants k_2' , k_4' , k_5 and k_5' in their kinetic scheme), but is the same as the recent scheme used by Tsiang[14] (who use a different approach[22,23] at modeling the system). The various functional groups, -A, -B and -A', at the ends of the molecules and internal linkages, -AB-, -A*B- and -A$^\#$B-, are also defined in this table. Since PAA can be present in two kinetically non-equivalent forms[14,15,24,25], a transformation from one to the other (Rxn. 5) is incorporated in this scheme. Only the -AB- internal linkage is able to cyclize in the curing stage through Rxn. 2. Rxns. 2-5 would be significant primarily in the curing stage, while Rxn. 1 would be most important in the first stage. The kinetic scheme is, thus, observed to include all the reactions (relevant to both stages).

The rate constants used in Table 1 are given by the Arrhenius equation

$$k_i \text{ (or } k_i') = A_i \exp(-E_i/RT) \qquad (1)$$

The (guess) values of the frequency factors, A_i, and activation energies, E_i, are given in Table 2 (in column a). These have been taken from Refs. 11 and 14 and are improved upon by using an optimal parameter estimation technique.

Table 1

Kinetic Scheme in Terms of Functional Groups

1) Polycondensation (Amidization):

$$— A + B — \quad \underset{k_1'}{\overset{k_1}{\rightleftharpoons}} \quad — AB —$$
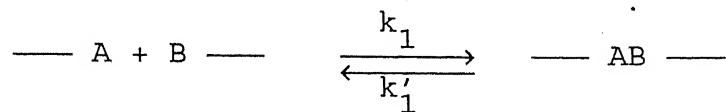
2) Imidization (Curing):

$$— AB — \quad \underset{k_2'}{\overset{k_2}{\rightleftharpoons}} \quad — A^*B — + W$$
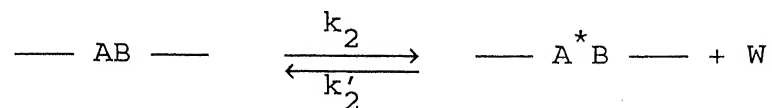
3) Hydrolysis of Polyamic Acid (Degradation):

$$— AB — + W \quad \xrightarrow{k_3'} \quad — A' + B —$$
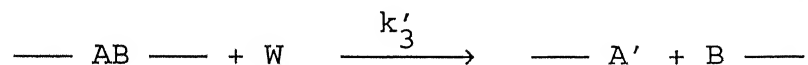
4) Hydrolysis of Anhydride Group :

$$— A + W \quad \underset{k_4'}{\overset{k_4}{\rightleftharpoons}} \quad — A'$$
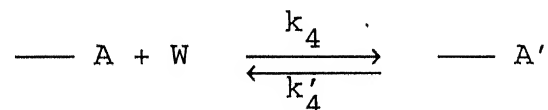
5) Transformation :

$$— AB — \quad \underset{k_5'}{\overset{k_5}{\rightleftharpoons}} \quad — A^{\#}B —$$

-A :

(Table 1 contd...b)

-A :

-B : $-NH_2$

-AB- :

-A' :

-A*B- :

-A#B- :

W : H_2O
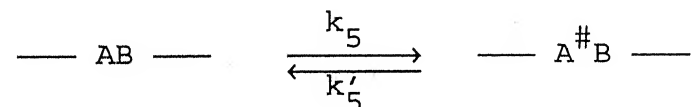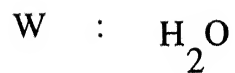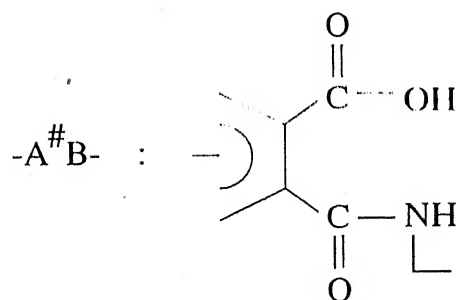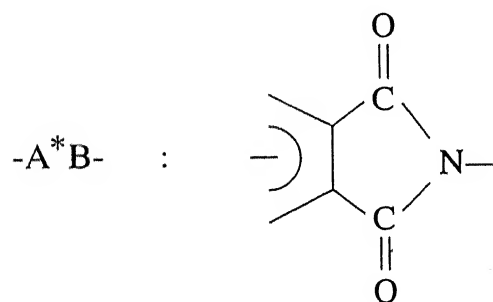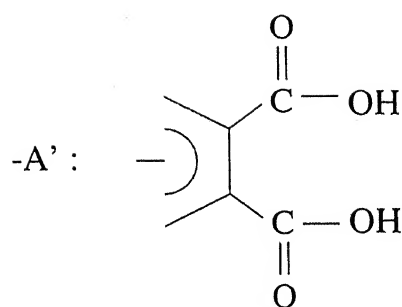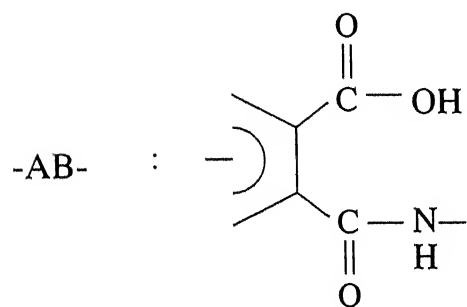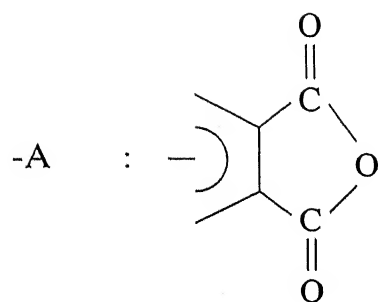
Table 2

Kinetic Parameters

Rate Constants	E_i^* (J/mol)	(a) A_i^* @ (Initial Guess)	(b) A_i (Best-fit Values)
k_1 $(m^3/mol-s)$	2.93×10^4	7.42×10^2 @	1.16×10^3
k_1' (s^{-1})	1.03×10^5	1.12×10^8	1.12×10^8
k_2 (s^{-1})	1.09×10^5	3.97×10^9	3.97×10^9
k_2' $(m^3/mol-s)$	1.50×10^5	2.08×10^{-4}	2.08×10^{-3}
k_3' $(m^3/mol-s)$	1.03×10^5	2.40×10^4	2.40×10^5
k_4 $(m^3/mol-s)$	5.27×10^4	5.86×10^4 @	1.03×10^5
k_4' (s^{-1})	7.62×10^4	8.65×10^6	8.65×10^6
k_5 (s^{-1})	9.63×10^4	2.60×10^7	2.60×10^7
k_5' (s^{-1})	9.63×10^4	2.60×10^7	2.60×10^7

* Ref. 14

@ Ref. 11

Before proceeding further, all the *molecular* species present in the reaction mass must be identified. The kinetic scheme of Table 1 suggests six sets of such species and these are defined in Table 3. In this table, -I- represents *any* internal group (-AB-, -A*B- or -A$^\#$B- , see Table 1). Each molecular species, e.g., $P_{n,AA}$, in this table clubs together a host of molecules having the same number of repeat units, n, but having different chemical structures at the internal linkages. Thus, the concentration, [$P_{n,AA}$], really represents a sum of the concentrations of all molecular species, $P_{n,AA,i}$, having n AA units and n-1 BB units (with both the ends being an unreacted dianhydride), but differing from one another in the sequential arrangements of internal units from among -AB-, -A*B- and -A$^\#$B-. These molecules range from one having all the 2(n-1) internal groups of the -AB- kind, to one having all 2(n-1) of the -A*B- kind, etc. Such a clubbing is necessary to keep the model tractable. Thus, the concentration of $P_{n,AA}$, for example, is given by

$$[P_{n,AA}] = \sum_{\text{all species},i} [P_{n,AA,i}] \text{ ,etc.} \qquad (2)$$

The kth moments (k = 0,1,2,...) of the various molecular species are also defined in Table 3. Again, the summation over all species having the same length, n, but different internal distributions of the -AB-, -A*B- and -A$^\#$B- groups, is accounted for by the use of the clubbed species (see Eq. 1). The number and weight average molecular weights, M_n and M_w, for this complex system have been obtained starting from the fundamental equations[8,9]

Table 3

Definition of Various Molecular Species, Moments

and Average Molecular Weights

Molecular Species[*]

Symbol	(a) Representation (schematic)	Number of			
		AA	BB	AA'	-I-
$P_{n,AA}$	AABBAA————AABBAA	n	n-1	0	2(n-1)
$P_{n,BB}$	BBAABB————BBAABB	n-1	n	0	2(n-1)
$P_{n,AB}$	AABBAA————BBAABB	n	n	0	2n-1
$P_{n,A'A}$	A'ABBAA————AABBAA	n-1	n-1	1	2(n-1)
$P_{n,A'A'}$	A'ABBAA————AABBAA'	n-2	n-1	2	2(n-1)
$P_{n,A'B}$	A'ABBAA————BBAABB	n-1	n	1	2n-1

[*] The total number of AA, AA' and BB (both at ends and in the inside) units in a molecule are listed above. The internal groups -I- (indicated as AB in column a above), could be either -AB-, -A[*]B-, or -A[#]B-, as defined in Table 1. Thus, $P_{n,AA}$, for example, clubs together several species having the same length and end groups, but with different internal groups.

(Table 3 contd...b)

k^{th} Moments of Various Molecular Species[**]

$$\lambda_{AA}^{k} \equiv \sum_{n=1}^{\infty} n^{k} P_{n,AA}$$

$$\lambda_{BB}^{k} \equiv \sum_{n=1}^{\infty} n^{k} P_{n,BB}$$

$$\lambda_{AB}^{k} \equiv \sum_{n=1}^{\infty} n^{k} P_{n,AB}$$

$$\lambda_{A'A}^{k} \equiv \sum_{n=1}^{\infty} n^{k} P_{n,A'A}$$

$$\lambda_{A'A'}^{k} \equiv \sum_{n=1}^{\infty} n^{k} P_{n,A'A'}$$

$$\lambda_{A'B}^{k} \equiv \sum_{n=1}^{\infty} n^{k} P_{n,A'B} \quad ; \quad k = 0,1,2, \ldots$$

[**] $P_{n,AA}$, etc., indicate concentrations here. Again, the moments club together molecules with different internal groups (-AB- , -A[*]B- and -A[#]B-). Note that k is a superscript and not an exponent.

Table 3 contd.

(Table 3 contd....c)

Average Molecular Weights

$$M_n \equiv \frac{\begin{array}{l}[(w_{AA} + w_{BB})\{\lambda^1_{AA} + \lambda^1_{BB} + \lambda^1_{AB} + \lambda^1_{A'A} + \lambda^1_{A'A'} + \lambda^1_{A'B}\} \\ - w_{AA}\{\lambda^0_{BB} + \lambda^0_{A'A} + \lambda^0_{A'B} + 2\lambda^0_{A'A'}\} - w_{BB}\{\lambda^0_{AA} + \lambda^0_{A'A} \\ + \lambda^0_{A'A'}\} + w_{A'A}\{\lambda^0_{A'A} + \lambda^0_{A'B} + 2\lambda^0_{A'A'}\}]\end{array}}{[\lambda^0_{AA} + \lambda^0_{BB} + \lambda^0_{AB} + \lambda^0_{A'A} + \lambda^0_{A'A'} + \lambda^0_{A'B}]}$$

$$M_w \equiv \frac{\begin{array}{l}[\, w^2_{AA}\{\lambda^2_{AA} + \lambda^2_{BB} - 2\lambda^1_{BB} + \lambda^0_{BB}\} + w^2_{BB}\{\lambda^2_{AA} + \lambda^2_{BB} \\ - 2\lambda^1_{AA} + \lambda^0_{AA}\} + 2w_{AA}w_{BB}\{\lambda^2_{AA} + \lambda^2_{BB} - \lambda^1_{AA} - \lambda^1_{BB}\} \\ + 2(w_{AA} + w_{BB})\{w_{A'A}(\lambda^1_{A'A} - \lambda^0_{A'A}) + (2w_{A'A} \\ - w_{AA})(\lambda^1_{A'A'} - \lambda^0_{A'A'}) + (w_{A'A} + w_{BB})(\lambda^1_{A'B} - \lambda^0_{A'B})\} \\ + (w_{AA} + w_{BB})^2\{\lambda^2_{AB} + \lambda^2_{A'A} + \lambda^2_{A'A'} + \lambda^2_{A'B} - 2\lambda^1_{A'A} \\ - 2\lambda^1_{A'A'} - 2\lambda^1_{A'B} + \lambda^0_{A'A} + \lambda^0_{A'A'} + \lambda^0_{A'B}\} + w^2_{A'A}\lambda^0_{A'A} \\ + (2w_{A'A} - w_{AA})^2\lambda^0_{A'A'} + (w_{A'A} + w_{BB})^2\lambda^0_{A'B}]\end{array}}{\begin{array}{l}[(w_{AA} + w_{BB})\{\lambda^1_{AA} + \lambda^1_{BB} + \lambda^1_{AB} + \lambda^1_{A'A} + \lambda^1_{A'A'} + \lambda^1_{A'B}\} \\ - w_{AA}\{\lambda^0_{BB} + \lambda^0_{A'A} + \lambda^0_{A'B} + 2\lambda^0_{A'A'}\} - w_{BB}\{\lambda^0_{AA} + \lambda^0_{A'A} \\ + \lambda^0_{A'A'}\} + w_{A'A}\{\lambda^0_{A'A} + \lambda^0_{A'B} + 2\lambda^0_{A'A'}\}]\end{array}}$$

$$PDI \equiv \frac{M_w}{M_n}$$

—— X ——

$$M_n = \sum_{\text{all species}} (\text{number fraction of } i^{th} \text{ species}) \times$$
$$(\text{molecular weight of } i^{th} \text{ species}) \qquad (a)$$

$$M_w = \sum_{\text{all species}} (\text{mass fraction of } i^{th} \text{ species}) \times$$
$$(\text{molecular weight of } i^{th} \text{ species}) \qquad (b)$$

$$(3)$$

The final expressions are given in Table 3.

The balance equations for a well-mixed batch reactor for the various groups shown in Table 1 are now developed. These can easily be written and are given in Table 4. The concentration of the internal linkages, [-I-], is the sum of the three concentrations, [-AB-], [-A*B-] and [-A#B-], and the balance equation for [-I-] can be obtained by summing up the corresponding three equations. The simplified equation for [-I-] is also given in Table 4. These equations can be integrated for isothermal operation (for a given set of rate constants and initial conditions) to obtain the concentrations of any group at any moment of time, t. The *overall* fractions of -AB- and -A*B- in -I- are defined as f_{AB} and f_{A^*B}, respectively. These can be computed at any value of t, and the fraction of -I- which are of the kind, -A#B-, can be obtained using

$$f_{A^\#B} = 1 - (f_{AB} + f_{A^*B}) \qquad (4)$$

The balance equations in Table 4 can give only partial information about the system. Mass balance equations for the individual (clubbed) species described in Table 3 need to be written before the equations for the moments of the chain length distribution can be obtained. These are summarized in Table 5. In these equations, great care has been taken to account for *all* the possibilities of formation and depletion of the individual

22

Table 4

Mass Balance Equations for the Groups in Table 1

$$\frac{d\,[-A]}{dt} = -k_1[-A][-B] + k_1'[-AB-] - k_4[-A][W] + k_4'[-A']$$

$$\frac{d\,[-B]}{dt} = -k_1[-A][-B] + k_1'[-AB-] + k_3'[W][-AB-]$$

$$\frac{d\,[-A']}{dt} = k_3'[W][-AB-] + k_4[W][-A] - k_4'[-A']$$

$$\frac{d\,[-AB-]}{dt} = k_1[-A][-B] - k_1'[-AB-] - k_2[-AB-] + k_2'[W][-A^*B-]$$
$$- k_3'[W][-AB-] - k_5[-AB-] + k_5'[-A^{\#}B-]$$

$$\frac{d\,[-A^*B-]}{dt} = k_2[-AB-] - k_2'[W][-A^*B-]$$

$$\frac{d\,[-A^{\#}B-]}{dt} = k_5[-AB-] - k_5'[-A^{\#}B-]$$

$$\frac{d\,[W]}{dt} = k_2[-AB-] - k_2'[W][-A^*B-] - k_3'[W][-AB-] - k_4[W][-A]$$
$$+ k_4'[-A']$$

Some Other Quantities

$$\frac{d\,[-I-]}{dt} \equiv \frac{d}{dt}\{\,[-AB-] + [-A^*B-] + [-A^{\#}B-]\,\}$$

$$= k_1[-A][-B] - k_1'[-AB-] - k_3'[W][-AB-]$$

Table 4 contd.

(Table 4 contd.....b)

$$f_{AB} \equiv \frac{[-AB-]}{[-I-]}$$

$$f_{A^*B} \equiv \frac{[-A^*B-]}{[-I-]}$$

$$f_{A^{\#}B} \equiv \frac{[-A^{\#}B-]}{[-I-]} = 1 - f_{AB} - f_{A^*B}$$

—— X ——

24

Table 5

Mass Balance Equations for the Molecular Species

in a Batch Reactor

$$\frac{dP_{n,AA}}{dt} = 2k_1\Delta_1 \sum_{r=1}^{n-1} P_{r,AA}P_{n-r,AB} - 2k_1P_{n,AA}\left[\sum_{m=1}^{\infty} P_{m,AB} + \sum_{m=1}^{\infty} P_{m,A'B} \right.$$

$$\left. + 2\sum_{m=1}^{\infty} P_{m,BB} \right] + k_1'f_{AB}\left[\sum_{m=n+1}^{\infty} P_{m,A'A} + 2\sum_{m=n+1}^{\infty} P_{m,AA} + \sum_{m=n}^{\infty} P_{m,AB} \right]$$

$$- 2k_1'f_{AB}(n-1)P_{n,AA} - 2k_3'f_{AB}W(n-1)P_{n,AA} - 2k_4WP_{n,AA}$$

$$+ k_4'P_{n,A'A}$$

$$\frac{dP_{n,BB}}{dt} = 2k_1\Delta_1 \sum_{r=1}^{n-1} P_{r,BB}P_{n-r,AB} - 2k_1P_{n,BB}\left[2\sum_{m=1}^{\infty} P_{m,AA} + \sum_{m=1}^{\infty} P_{m,AB} \right.$$

$$\left. + \sum_{m=1}^{\infty} P_{m,A'A} \right] + k_1'f_{AB}\left[2\sum_{m=n+1}^{\infty} P_{m,BB} + \sum_{m=n}^{\infty} P_{m,AB} + \sum_{m=n}^{\infty} P_{m,A'B} \right]$$

$$- 2k_1'f_{AB}(n-1)P_{n,BB} + k_3'f_{AB}W\left[2\sum_{m=n+1}^{\infty} P_{m,BB} + \sum_{m=n}^{\infty} P_{m,AB} \right.$$

$$\left. + \sum_{m=n}^{\infty} P_{m,A'B} \right] - 2k_3'f_{AB}W(n-1)P_{n,BB}$$

(Table 5 contd....b)

$$\frac{dP_{n,AB}}{dt} = 4k_1 \sum_{m=1}^{n} P_{m,AA} P_{n-m+1,BB} + k_1 \Delta_1 \sum_{m=1}^{n-1} P_{m,AB} P_{n-m,AB}$$

$$- k_1 P_{n,AB} \left[2\sum_{m=1}^{\infty} P_{m,AA} + 2\sum_{m=1}^{\infty} P_{m,BB} + 2\sum_{m=1}^{\infty} P_{m,AB} + \sum_{m=1}^{\infty} P_{m,A'A} \right.$$

$$+ \left. \sum_{m=1}^{\infty} P_{m,A'B} \right] + k_1' f_{AB} \sum_{m=n+1}^{\infty} \{2P_{m,AA} + 2P_{m,BB} + 2P_{m,AB} + P_{m,A'A}$$

$$+ P_{m,A'B}\} - k_1' f_{AB} (2n-1) P_{n,AB} + k_3' f_{AB} W \sum_{m=n+1}^{\infty} \{2P_{m,AA}$$

$$+ P_{m,AB} + P_{m,A'A}\} - k_3' f_{AB} W (2n-1) P_{n,AB} - k_4 W P_{n,AB}$$

$$+ k_4' P_{n,A'B}$$

$$\frac{dP_{n,A'A}}{dt} = - k_1 P_{n,A'A} \left[2\sum_{m=1}^{\infty} P_{m,BB} + \sum_{m=1}^{\infty} P_{m,AB} + \sum_{m=1}^{\infty} P_{m,A'B} \right]$$

$$+ 2k_1' \Delta_1 \sum_{m=1}^{n-1} P_{m,A'B} P_{n-m,AA} + k_1 \Delta_1 \sum_{m=1}^{n-1} P_{m,A'A} P_{n-m,AB}$$

$$- 2k_1' f_{AB} (n-1) P_{n,A'A} + k_1' f_{AB} \left[\sum_{m=n+1}^{\infty} P_{m,A'A} + 2\sum_{m=n+1}^{\infty} P_{m,A'A'} \right.$$

$$+ \left. \sum_{m=n}^{\infty} P_{m,A'B} \right] - 2k_3' f_{AB} (n-1) W P_{n,A'A} + k_3' f_{AB} W \left[2\sum_{m=n+1}^{\infty} P_{m,AA} \right.$$

$$+ \left. \sum_{m=n}^{\infty} P_{m,AB} + \sum_{m=n+1}^{\infty} P_{m,A'A} \right] - k_4 W P_{n,A'A} + 2k_4 W P_{n,AA}$$

$$+ k_4' \left[2P_{n,A'A'} - P_{n,A'A} \right]$$

Table 5 contd.

(Table 5 contd....c)

$$\frac{dP_{n,A'A'}}{dt} = k_1\Delta_1 \sum_{m=1}^{n-1} P_{m,A'A}P_{n-m,A'B} - 2k_1' f_{AB}(n-1)P_{n,A'A'}$$

$$- 2k_3' f_{AB}W(n-1)P_{n,A'A'} + k_3' f_{AB}W\left[\sum_{m=n}^{\infty} P_{m,A'B} \right.$$

$$\left. + \sum_{m=n+1}^{\infty} P_{m,A'A} + 2\sum_{m=n+1}^{\infty} P_{m,A'A'} \right] + k_4 W P_{n,A'A} - 2k_4' P_{n,A'A'}$$

$$\frac{dP_{n,A'B}}{dt} = -k_1 P_{n,A'B}\left[2\sum_{m=1}^{\infty} P_{m,AA} + \sum_{m=1}^{\infty} P_{m,AB} + \sum_{m=1}^{\infty} P_{m,A'A} \right]$$

$$+ k_1\Delta_1 \sum_{m=1}^{n-1} P_{m,A'B}P_{n-m,AB} + 2k_1\sum_{m=1}^{n} P_{m,A'A}P_{n-m+1,BB}$$

$$- k_1' f_{AB}(2n-1)P_{n,A'B} + k_1' f_{AB}\left[\sum_{m=n+1}^{\infty} P_{m,A'A} + \sum_{m=n+1}^{\infty} P_{m,A'B} \right.$$

$$\left. + 2\sum_{m=n+1}^{\infty} P_{m,A'A'} \right] - k_3' f_{AB}W(2n-1)P_{n,A'B}$$

$$+ k_3' f_{AB}W\left[\sum_{m=n+1}^{\infty} P_{m,AB} + 2\sum_{m=n+1}^{\infty} P_{m,BB} + \sum_{m=n+1}^{\infty} P_{m,A'A} \right.$$

$$\left. + 2\sum_{m=n+1}^{\infty} P_{m,A'B} + 2\sum_{m=n+1}^{\infty} P_{m,A'A'} \right] + k_4 W P_{n,AB} - k_4' P_{n,A'B}$$

(Table 5 contd....d)

$$\frac{dW}{dt} = - k_3' f_{AB} W \left[\sum_{n=1}^{\infty} (2n-2) \{ P_{n,AA} + P_{n,BB} + P_{n,A'A} + P_{n,A'A'} \} \right]$$

$$- k_3' f_{AB} W \left[\sum_{n=1}^{\infty} (2n-1) \{ P_{n,AB} + P_{n,A'B} \} \right] - k_4 W \left[\sum_{n=1}^{\infty} \{ 2P_{n,AA} \right.$$

$$\left. + P_{n,AB} + P_{n,A'A} \} \right] + k_4' \left[\sum_{n=1}^{\infty} \{ P_{n,A'A} + P_{n,A'B} \right.$$

$$\left. + 2P_{n,A'A'} \} \right] + (k_2 f_{AB} - k_2' f_{A^*B} W) \left[\sum_{n=1}^{\infty} (2n-2) \{ P_{n,AA} \right.$$

$$\left. + P_{n,BB} + P_{n,A'A} + P_{n,A'A'} \} + \sum_{n=1}^{\infty} (2n-1) \{ P_{n,AB} \right.$$

$$\left. + P_{n,A'B} \} \right]$$

---

a. $\Delta_1 = 0$ if $n = 1$

$= 1$ if $n > 1$

b. f_{AB} and f_{A^*B} to be obtained from integration of (all) the equations in Table 4.

c. notation [,] for concentrations are not being used in this table for the sake of brevity.

— x —

molecular species which the kinetic scheme (in terms of *groups*) in Table 1 represents. The terms in the first equation in Table 5 (for $dP_{n,AA}/dt$) are explained to illustrate the several assumptions and concepts involved. The first term, $2k_1\Delta_1\sum_{r=1}^{n-1}P_{r,AA}P_{n-r,AB}$, represents the formation of $P_{n,AA}$ by the reaction between A and B end groups of the shorter $P_{r,AA}$ and $P_{n-r,AB}$ molecules, the factor of 2 accounting for the two possibilities (2 A groups of $P_{r,AA}$ reacting with the single B group of $P_{n-r,AB}$). The next three terms involve the depletion of $P_{n,AA}$ by the reaction of two of its end A groups with the end B groups of *all* $P_{m,AB}$, $P_{m,A'B}$ and $P_{m,BB}$ molecules. The reaction between $P_{n,AA}$ with $P_{m,BB}$ involves four possibilities, which is reflected by the multiplication factor. The next three terms involving $k_1'f_{AB}$ account for the formation of $P_{n,AA}$ by the scission (due to the reverse Rxn. 1) at an appropriately placed internal -AB- link of a higher length $P_{m,A'A}$, $P_{m,AA}$ or $P_{m,AB}$ molecule (m > n or n+1). While only a single molecule of $P_{n,AA}$ is generated when $P_{m,A'A}$ and $P_{m,AB}$ undergo this reaction (the other molecule being $P_{m-n,A'B}$ and $P_{m-n,AB}$, respectively), there are two locations of -AB- in $P_{m,AA}$ which could lead to the formation of $P_{n,AA}$ (the other molecule produced being $P_{m-n,AA}$). The factor, f_{AB}, used in these terms is the probability that the appropriate internal location at which this chain scission is to take place, is indeed an -AB- linkage rather than an $-A^*B-$ or $-A^\#B-$. It is being assumed that the *overall* fraction of -I- groups being -AB- is the same as the *local* probability of finding an -AB- group at the right location in *any* of the larger molecules ($P_{m,A'A}$, $P_{m,AA}$ and $P_{m,AB}$). Such an approximation that the overall probability is the same as

the local probability, independent of the length, m, is quite commonly made in polymer reaction engineering,[9] particularly for the polymerization of phenol and melamine formaldehyde.[26] The next term, $-2k_1' f_{AB}(n-1)P_{n,AA}$, represents the depletion of $P_{n,AA}$ by the reverse step of Rxn. 1 (Table 1) at any of its 2(n-1) internal locations which happen to be of the -AB- kind. Again, the probability that *any* of these internal locations is -AB-, as opposed to $-A^*B-$ or $-A^\#B-$, is assumed to be f_{AB}, the overall fraction of internal locations which are of the -AB- type. The term, $-2k_3' f_{AB}W(n-1)P_{n,AA}$, can be similarly explained for Rxn. 3. The last two terms in this equation correspond to the depletion (two possibilities at the two -A end groups) and formation (only a single possibility) of $P_{n,AA}$ and $P_{n,A'A}$ by the forward and reverse steps of Rxn. 4 in Table 1. All other equations in Table 5 can be similarly explained, using the above discussion. The equations in Table 5 were checked out by two independent derivations. In addition, using $k_i = k_i' = 0$ (i≠1), it was found that these equations reduce to those for simple AA + BB reversible polymerization (without formation of the condensation byproduct). These give us confidence on the correctness of these relatively complex equations.

The equations in Table 5 can be appropriately summed up (using the definitions in Table 3) to give ordinary differential equations (ODEs) for the several moments (k=0, 1 and 2). Several summation identities given in Chap. 1 in Ref. 9 (besides a few others which had to be developed) proved helpful. The final equations for the moments are given in Table 6. It is observed that the equations for several of the second moments require third

Table 6

Moment Equations in a Batch Reactor

$$\frac{d\lambda_{AA}^0}{dt} = -k_1(4\lambda_{AA}^0\lambda_{BB}^0 + 2\lambda_{AA}^0\lambda_{A'B}^0) + k_1'f_{AB}(\lambda_{AB}^1 + \lambda_{A'A}^1 - \lambda_{A'A}^0)$$

$$-2k_3'f_{AB}W(\lambda_{AA}^1 - \lambda_{AA}^0) - 2k_4W\lambda_{AA}^0 + k_4'\lambda_{A'A}^0$$

$$\frac{d\lambda_{BB}^0}{dt} = -k_1(4\lambda_{AA}^0\lambda_{BB}^0 + 2\lambda_{BB}^0\lambda_{A'A}^0) + k_1'f_{AB}(\lambda_{AB}^1 + \lambda_{A'B}^1)$$

$$+k_3'f_{AB}W(\lambda_{AB}^1 + \lambda_{A'B}^1)$$

$$\frac{d\lambda_{AB}^0}{dt} = k_1(4\lambda_{AA}^0\lambda_{BB}^0 - \lambda_{AB}^0\lambda_{AB}^0 - 2\lambda_{AB}^0\lambda_{BB}^0 - 2\lambda_{AB}^0\lambda_{AA}^0 - \lambda_{AB}^0\lambda_{A'B}^0$$

$$- \lambda_{AB}^0\lambda_{A'A}^0) + k_1'f_{AB}(2\lambda_{AA}^1 + 2\lambda_{BB}^1 + \lambda_{A'A}^1 + \lambda_{A'B}^1 - \lambda_{AB}^0$$

$$- 2\lambda_{AA}^0 - 2\lambda_{BB}^0 - \lambda_{A'A}^0 - \lambda_{A'B}^0) + k_3'f_{AB}W(2\lambda_{AA}^1 + \lambda_{A'A}^1$$

$$- \lambda_{AB}^1 - 2\lambda_{AA}^0 - \lambda_{A'A}^0) - k_4W\lambda_{AB}^0 + k_4'\lambda_{A'B}^0$$

$$\frac{d\lambda_{A'A}^0}{dt} = k_1(2\lambda_{AA}^0\lambda_{A'B}^0 - 2\lambda_{BB}^0\lambda_{A'A}^0 - \lambda_{A'A}^0\lambda_{A'B}^0) + k_1'f_{AB}(2\lambda_{A'A'}^1$$

$$+ \lambda_{A'B}^1 - \lambda_{A'A}^1 + \lambda_{A'A}^0 - 2\lambda_{A'A'}^0) + k_3'f_{AB}W(2\lambda_{AA}^1 + \lambda_{AB}^1$$

$$- \lambda_{A'A}^1 + \lambda_{A'A}^0 - 2\lambda_{AA}^0) + k_4W(2\lambda_{AA}^0 - \lambda_{A'A}^0) + k_4'(2\lambda_{A'A'}^0$$

$$- \lambda_{A'A}^0)$$

$$\frac{d\lambda_{A'A'}^0}{dt} = k_1\lambda_{A'A}^0\lambda_{A'B}^0 - 2k_1'f_{AB}(\lambda_{A'A'}^1 - \lambda_{A'A'}^0) + k_3'f_{AB}W(\lambda_{A'A}^1$$

$$+ \lambda_{A'B}^1 - \lambda_{A'A}^0) + k_4W\lambda_{A'A}^0 - 2k_4'\lambda_{A'A'}^0$$

(Table 6 contd...b)

$$\frac{d\lambda^0_{A'B}}{dt} = k_1(2\lambda^0_{BB}\lambda^0_{A'A} - 2\lambda^0_{AA}\lambda^0_{A'B} - \lambda^0_{A'A}\lambda^0_{A'B}) + k'_1 f_{AB}(2\lambda^1_{A'A'}$$

$$+ \lambda^1_{A'A} - \lambda^1_{A'B} - \lambda^0_{A'A} - 2\lambda^0_{A'A'}) + k'_3 f_{AB}W(2\lambda^1_{BB} + \lambda^1_{AB}$$

$$+ \lambda^1_{A'A} + 2\lambda^1_{A'A'} - 2\lambda^0_{BB} - \lambda^0_{AB} - \lambda^0_{A'A} - 2\lambda^0_{A'A'} - \lambda^0_{A'B})$$

$$+ k_4 W\lambda^0_{AB} - k'_4\lambda^0_{A'B}$$

$$\frac{d\lambda^1_{AA}}{dt} = k_1(2\lambda^0_{AA}\lambda^1_{AB} - 4\lambda^1_{AA}\lambda^0_{BB} - 2\lambda^1_{AA}\lambda^0_{A'B}) + k'_1 f_{AB}(0.5\lambda^2_{AB}$$

$$+ 0.5\lambda^2_{A'A} - \lambda^2_{AA} + \lambda^1_{AA} + 0.5\lambda^1_{AB} - 0.5\lambda^1_{A'A})$$

$$- 2k'_3 Wf_{AB}(\lambda^2_{AA} - \lambda^1_{AA}) - 2k_4 W\lambda^1_{AA} + k'_4\lambda^1_{A'A}$$

$$\frac{d\lambda^1_{BB}}{dt} = k_1(2\lambda^0_{BB}\lambda^1_{AB} - 4\lambda^0_{AA}\lambda^1_{BB} - 2\lambda^0_{A'A}\lambda^1_{BB}) + k'_1 f_{AB}W(0.5\lambda^2_{AB}$$

$$+ 0.5\lambda^2_{A'B} - \lambda^2_{BB} + \lambda^1_{BB} + 0.5\lambda^1_{AB} + 0.5\lambda^1_{A'B})$$

$$+ k'_3 f_{AB}W(0.5\lambda^2_{AB} + 0.5\lambda^2_{A'B} - \lambda^2_{BB} + \lambda^1_{BB} + 0.5\lambda^1_{AB}$$

$$+ 0.5\lambda^1_{A'B})$$

$$\frac{d\lambda^1_{AB}}{dt} = k_1(4\lambda^0_{AA}\lambda^1_{BB} + 4\lambda^0_{BB}\lambda^1_{AA} - 4\lambda^0_{AA}\lambda^0_{BB} - \lambda^0_{A'A}\lambda^1_{AB} - 2\lambda^0_{AA}\lambda^1_{AB}$$

$$- \lambda^0_{A'B}\lambda^1_{AB} - 2\lambda^0_{BB}\lambda^1_{AB}) + k'_1 f_{AB}(\lambda^2_{AA} + \lambda^2_{BB} - \lambda^2_{AB}$$

$$+ 0.5\lambda^2_{A'A} + 0.5\lambda^2_{A'B} - \lambda^1_{AA} - \lambda^1_{BB} - 0.5\lambda^1_{A'A} - 0.5\lambda^1_{A'B})$$

$$+ k'_3 f_{AB}W(\lambda^2_{AA} - 1.5\lambda^2_{AB} + 0.5\lambda^2_{A'A} - \lambda^1_{AA} + 0.5\lambda^1_{AB}$$

$$- 0.5\lambda^1_{A'A}) - k_4 W\lambda^1_{AB} + k'_4\lambda^1_{A'B}$$

Table 6 contd.

(Table 6 contd....c)

$$\frac{d\lambda^1_{A'A}}{dt} = k_1(2\lambda^0_{AA}\lambda^1_{A'B} + 2\lambda^0_{A'B}\lambda^1_{AA} - 2\lambda^0_{BB}\lambda^1_{A'A} - \lambda^0_{A'B}\lambda^1_{A'A}$$

$$+ \lambda^0_{A'A}\lambda^1_{AB}) + k'_1 f_{AB}(\lambda^2_{A'A'} + 0.5\lambda^2_{A'B} - 1.5\lambda^2_{A'A}$$

$$- \lambda^1_{A'A'} + 0.5\lambda^1_{A'B} + 1.5\lambda^1_{A'A}) + k'_3 f_{AB} W(\lambda^2_{AA}$$

$$+ 0.5\lambda^2_{AB} - 1.5\lambda^2_{A'A} - \lambda^1_{AA} + 0.5\lambda^1_{AB} + 1.5\lambda^1_{A'A})$$

$$+ k_4 W(2\lambda^1_{AA} - \lambda^1_{A'A}) + k'_4(2\lambda^1_{A'A'} - \lambda^1_{A'A})$$

$$\frac{d\lambda^1_{A'A'}}{dt} = k_1(\lambda^0_{A'A}\lambda^1_{A'B} + \lambda^0_{A'B}\lambda^1_{A'A}) - 2k'_1 f_{AB}(\lambda^2_{A'A'} - \lambda^1_{A'A'})$$

$$+ k'_3 f_{AB} W(0.5\lambda^2_{A'A} + 0.5\lambda^2_{A'B} - \lambda^2_{A'A'} + \lambda^1_{A'A'}$$

$$- 0.5\lambda^1_{A'A} + 0.5\lambda^1_{A'B}) + k_4 W\lambda^1_{A'A} - 2k'_4\lambda^1_{A'A'}$$

$$\frac{d\lambda^1_{A'B}}{dt} = k_1(2\lambda^0_{A'A}\lambda^1_{BB} + 2\lambda^0_{BB}\lambda^1_{A'A} - 2\lambda^0_{BB}\lambda^0_{A'A} - 2\lambda^0_{AA}\lambda^1_{A'B}$$

$$- \lambda^0_{A'A}\lambda^1_{A'B} + \lambda^0_{A'B}\lambda^1_{AB}) + k'_1 f_{AB}(0.5\lambda^2_{A'A} + \lambda^2_{A'A'} - 1.5\lambda^2_{A'B}$$

$$+ 0.5\lambda^1_{A'B} - 0.5\lambda^1_{A'A} - \lambda^1_{A'A'}) + k'_3 f_{AB} W(\lambda^2_{BB} + 0.5\lambda^2_{AB}$$

$$+ 0.5\lambda^2_{A'A} - \lambda^2_{A'B} + \lambda^2_{A'A'} - \lambda^1_{BB} - 0.5\lambda^1_{A'A} - 0.5\lambda^1_{AB}$$

$$- \lambda^1_{A'A'}) + k_4 W\lambda^1_{AB} - k'_4\lambda^1_{A'B}$$

$$\frac{d\lambda^2_{AA}}{dt} = k_1(2\lambda^0_{AA}\lambda^2_{AB} + 4\lambda^1_{AA}\lambda^1_{AB} - 4\lambda^0_{BB}\lambda^2_{AA} - 2\lambda^0_{A'B}\lambda^2_{AA})$$

$$+ k'_1 f_{AB}(\tfrac{1}{3}\lambda^3_{AB} + \tfrac{1}{3}\lambda^3_{A'A} - \tfrac{4}{3}\lambda^3_{AA} + \lambda^2_{AA} + 0.5\lambda^2_{AB}$$

$$- 0.5\lambda^2_{A'A} + \tfrac{1}{3}\lambda^1_{AA} + \tfrac{1}{6}\lambda^1_{AB} + \tfrac{1}{6}\lambda^1_{A'A}) - 2k'_3 f_{AB} W(\lambda^3_{AA}$$

$$- \lambda^2_{AA}) - 2k_4 W\lambda^2_{AA} + k'_4\lambda^2_{A'A}$$

33

(Table 6 contd....d)

$$\frac{d\lambda_{BB}^2}{dt} = k_1(2\lambda_{BB}^0\lambda_{AB}^2 + 4\lambda_{BB}^1\lambda_{AB}^1 - 4\lambda_{AA}^0\lambda_{BB}^2 - 2\lambda_{A'A}^0\lambda_{BB}^2)$$

$$+ k_1'f_{AB}(\frac{1}{3}\lambda_{AB}^3 + \frac{1}{3}\lambda_{A'B}^3 - \frac{4}{3}\lambda_{BB}^3 + \lambda_{BB}^2 + 0.5\lambda_{AB}^2$$

$$+ 0.5\lambda_{A'B}^2 + \frac{1}{3}\lambda_{BB}^1 + \frac{1}{6}\lambda_{AB}^1 + \frac{1}{6}\lambda_{A'B}^1) + k_3'f_{AB}W(\frac{1}{3}\lambda_{AB}^3$$

$$+ \frac{1}{3}\lambda_{A'B}^3 - \frac{4}{3}\lambda_{BB}^3 + \lambda_{BB}^2 + 0.5\lambda_{AB}^2 + 0.5\lambda_{A'B}^2 + \frac{1}{3}\lambda_{BB}^1$$

$$+ \frac{1}{6}\lambda_{AB}^1 + \frac{1}{6}\lambda_{A'B}^1)$$

$$\frac{d\lambda_{AB}^2}{dt} = k_1(4\lambda_{AA}^0\lambda_{BB}^2 + 4\lambda_{BB}^0\lambda_{AA}^2 + 8\lambda_{AA}^1\lambda_{BB}^1 + 4\lambda_{AA}^0\lambda_{BB}^0$$

$$- 8\lambda_{BB}^0\lambda_{AA}^1 - 8\lambda_{AA}^0\lambda_{BB}^1 - 2\lambda_{BB}^0\lambda_{AB}^2 - 2\lambda_{AA}^0\lambda_{AB}^2 - \lambda_{A'B}^0\lambda_{AB}^2$$

$$- \lambda_{A'A}^0\lambda_{AB}^2 + 2\lambda_{AB}^1\lambda_{AB}^1) + k_1'f_{AB}(\frac{2}{3}\lambda_{BB}^3 + \frac{1}{3}\lambda_{A'A}^3$$

$$+ \frac{1}{3}\lambda_{A'B}^3 - \lambda_{BB}^2 - 0.5\lambda_{A'A}^2 - 0.5\lambda_{A'B}^2 + \frac{1}{3}\lambda_{BB}^1 + \frac{1}{6}\lambda_{A'A}^1$$

$$+ \frac{1}{6}\lambda_{A'B}^1 + \frac{2}{3}\lambda_{AA}^3 - \frac{4}{3}\lambda_{AB}^3 - \lambda_{AA}^2 + \frac{1}{3}\lambda_{AB}^1 + \frac{1}{3}\lambda_{AA}^1)$$

$$+ k_3'f_{AB}W(\frac{2}{3}\lambda_{AA}^3 - \frac{5}{3}\lambda_{AB}^3 + \frac{1}{3}\lambda_{A'A}^3 - \lambda_{AA}^2 + 0.5\lambda_{AB}^2$$

$$- 0.5\lambda_{A'A}^2 + \frac{1}{3}\lambda_{AA}^1 + \frac{1}{6}\lambda_{AB}^1 + \frac{1}{6}\lambda_{A'A}^1) - k_4W\lambda_{AB}^2$$

$$+ k_4'\lambda_{A'B}^2$$

$$\frac{d\lambda_{A'A}^2}{dt} = k_1(2\lambda_{AA}^0\lambda_{A'B}^2 + 2\lambda_{A'B}^0\lambda_{AA}^2 + 4\lambda_{AA}^1\lambda_{A'B}^1 + \lambda_{A'A}^0\lambda_{AB}^2$$

$$+ 2\lambda_{AB}^1\lambda_{A'A}^1 - 2\lambda_{BB}^0\lambda_{A'A}^2 - \lambda_{A'B}^0\lambda_{A'A}^2) + k_1'f_{AB}(\frac{2}{3}\lambda_{A'A'}^3$$

$$- \frac{5}{3}\lambda_{A'A}^3 + \frac{1}{3}\lambda_{A'B}^3 - \lambda_{A'A'}^2 + 1.5\lambda_{A'A}^2 + 0.5\lambda_{A'B}^2 + \frac{1}{3}\lambda_{A'A'}^1$$

$$+ \frac{1}{6}\lambda_{A'A}^1 + \frac{1}{6}\lambda_{A'B}^1) + k_3'f_{AB}W(\frac{2}{3}\lambda_{AA}^3 + \frac{1}{3}\lambda_{AB}^3 - \frac{5}{3}\lambda_{A'A}^3$$

$$- \lambda_{AA}^2 + 0.5\lambda_{AB}^2 + 1.5\lambda_{A'A}^2 + \frac{1}{3}\lambda_{AA}^1 + \frac{1}{6}\lambda_{AB}^1 + \frac{1}{6}\lambda_{A'A}^1)$$

$$+ k_4W(2\lambda_{AA}^2 - \lambda_{A'A}^2) + k_4'(2\lambda_{A'A'}^2 - \lambda_{A'A}^2)$$

Table 6 contd.

(Table 6 contd.....e)

$$\frac{d\lambda^2_{A'A'}}{dt} = k_1(\lambda^0_{A'A}\lambda^2_{A'B} + \lambda^0_{A'B}\lambda^2_{A'A} + 2\lambda^1_{A'A}\lambda^1_{A'B}) - 2k'_1 f_{AB}(\lambda^3_{A'A'}$$

$$- \lambda^2_{A'A'}) + k'_3 f_{AB}W(\frac{1}{3}\lambda^3_{A'A} - \frac{4}{3}\lambda^3_{A'A'} + \frac{1}{3}\lambda^3_{A'B}$$

$$- 0.5\lambda^2_{A'A} + \lambda^2_{A'A'} + 0.5\lambda^2_{A'B} + \frac{1}{6}\lambda^1_{A'A} + \frac{1}{3}\lambda^1_{A'A'}$$

$$+ \frac{1}{6}\lambda^1_{A'B}) + k_4 W\lambda^2_{A'A} - 2k'_4\lambda^2_{A'A'}$$

$$\frac{d\lambda^2_{A'B}}{dt} = k_1(2\lambda^0_{A'A}\lambda^2_{BB} + 2\lambda^0_{BB}\lambda^2_{A'A} + 4\lambda^1_{BB}\lambda^1_{A'A} - 4\lambda^0_{BB}\lambda^1_{A'A} - 4\lambda^0_{A'A}\lambda^1_{BB}$$

$$+ 2\lambda^0_{BB}\lambda^0_{A'A} - 2\lambda^0_{AA}\lambda^2_{A'B} - \lambda^0_{A'A}\lambda^2_{A'B} + \lambda^0_{A'B}\lambda^2_{AB} + 2\lambda^1_{AB}\lambda^1_{A'B})$$

$$+ k'_1 f_{AB}(\frac{1}{3}\lambda^3_{A'A} + \frac{2}{3}\lambda^3_{A'A'} - \frac{5}{3}\lambda^3_{A'B} - 0.5\lambda^2_{A'A} - \lambda^2_{A'A'}$$

$$+ 0.5\lambda^2_{A'B} + \frac{1}{6}\lambda^1_{A'A} + \frac{1}{3}\lambda^1_{A'A'} + \frac{1}{6}\lambda^1_{A'B}) + k'_3 f_{AB}W(\frac{2}{3}\lambda^3_{BB}$$

$$+ \frac{1}{3}\lambda^3_{AB} + \frac{1}{3}\lambda^3_{A'A} + \frac{2}{3}\lambda^3_{A'A'} - \frac{4}{3}\lambda^3_{A'B} - \lambda^2_{BB} - 0.5\lambda^2_{AB}$$

$$- 0.5\lambda^2_{A'A} - \lambda^2_{A'A'} + \frac{1}{3}\lambda^1_{BB} + \frac{1}{6}\lambda^1_{AB} + \frac{1}{6}\lambda^1_{A'A} + \frac{1}{3}\lambda^1_{A'A'}$$

$$+ \frac{1}{3}\lambda^1_{A'B}) + k_4 W\lambda^2_{AB} - k'_4\lambda^2_{A'B}$$

Moment Closure Equations For ith Species

$$\lambda^3_i = \frac{\lambda^2_i(2\lambda^2_i\lambda^0_i - \lambda^1_i\lambda^1_i)}{\lambda^1_i\lambda^0_i}$$

(i = AA, BB, AB, A'A, A'A', A'B)

—— X ——

35

moments. Thus, we have a hierarchy of infinite equations. A standard technique in polymer reaction engineering[8,9] is to break this hierarchy by using closure conditions. The closure equation which has been found to be quite successful for nylon 6, polyester, polyethylene and polyphenylene oxide[27] reaction systems, is tried here. This is also included in Table 6.

The following additional checks were made on the equations derived, to ensure that these were free of errors:

1) In Table 7, several groups (end as well as internal) have been written in terms of the various moments of the molecular species. Using these equalities with the equations of Table 6, we can obtain expressions for the rate equations *analytically*. We obtained the same equations as given in Table 4 (which were obtained using a functional group description, rather than a molecular species approach).

2) In a batch reactor, the total number of repeat units, AA, BB or AA', should be the same at any t as at t=0. Using Table 3, it is possible to obtain an equation for the total number of each of these repeat units in terms of the various moments. It is found that the rate of formation of each of these repeat unit is zero, as expected.

These two checks were sufficient to confirm the correctness of the mass balance and moment equations in Tables 5 and 6.

The equations in Tables 4 and 6 form a complete set of ODEs (initial value problems -- IVPs), which can be integrated for any given set of initial conditions (feed values). The numerical technique used to integrate these equations is Gear's algorithm.[28] The NAG library routine, D02EBF, which has a built-in step size

Table 7

Groups in Terms of Moments

$$[-A] \equiv 2\sum_{n=1}^{\infty} P_{n,AA} + \sum_{n=1}^{\infty} P_{n,AB} + \sum_{n=1}^{\infty} P_{n,A'A}$$

$$= 2\lambda_{AA}^{0} + \lambda_{AB}^{0} + \lambda_{A'A}^{0}$$

$$[-B] \equiv 2\sum_{n=1}^{\infty} P_{n,BB} + \sum_{n=1}^{\infty} P_{n,AB} + \sum_{n=1}^{\infty} P_{n,A'B}$$

$$= 2\lambda_{BB}^{0} + \lambda_{AB}^{0} + \lambda_{A'B}^{0}$$

$$[-A'] \equiv 2\sum_{n=1}^{\infty} P_{n,A'A'} + \sum_{n=1}^{\infty} P_{n,A'B} + \sum_{n=1}^{\infty} P_{n,A'A}$$

$$= 2\lambda_{A'A'}^{0} + \lambda_{A'B}^{0} + \lambda_{A'A}^{0}$$

$$[-I-] \equiv \sum_{n=1}^{\infty} \Big[2(n-1)\{P_{n,AA} + P_{n,BB} + P_{n,A'A} + P_{n,A'A'}\}$$

$$+ (2n-1)\{P_{n,AB} + P_{n,A'B}\}\Big]$$

$$= 2(\lambda_{AA}^{1} + \lambda_{BB}^{1} + \lambda_{AB}^{1} + \lambda_{A'A}^{1} + \lambda_{A'B}^{1} + \lambda_{A'A'}^{1})$$

$$- 2(\lambda_{AA}^{0} + \lambda_{BB}^{0} + \lambda_{A'A}^{0} + \lambda_{A'A'}^{0}) - (\lambda_{A'B}^{0} + \lambda_{AB}^{0})$$

$$[-COOH] \equiv 2[-A'] + (1-f_{A}{}^*{}_{B})[-I-]$$

$$= 2(2\lambda_{A'A'}^{0} + \lambda_{A'B}^{0} + \lambda_{A'A}^{0}) + (1-f_{A}{}^*{}_{B})\{2(\lambda_{AA}^{1} + \lambda_{BB}^{1}$$

$$+ \lambda_{AB}^{1} + \lambda_{A'A}^{1} + \lambda_{A'B}^{1} + \lambda_{A'A'}^{1}) - 2(\lambda_{AA}^{0} + \lambda_{BB}^{0}$$

$$+ \lambda_{A'A}^{0} + \lambda_{A'A'}^{0}) - (\lambda_{A'B}^{0} + \lambda_{AB}^{0})\}$$

—— X ——

control algorithm and is particularly useful for stiff systems, is used (with a tolerance, TOL, of 10^{-7}) for this purpose on an HP 9000/850 S computer system. Changing the value of the parameter, TOL, led to almost identical results. The two checks described above were also made with the computer code to ensure the correctness of the program (referred to as the simulation program).

Our set of modeling equations and our approach differ from the two models currently being used. In one of these,[11-13] the stochastic theory of chain branching processes of Gordon et al.[29,30] has been used. It is difficult to accomodate mass and heat transfer aspects in such theories. The other approach uses the results of Kilkson,[23,24] who develop expressions for only the final values of the average molecular weights for *irreversible* AA + BB condensation polymerization, in which all of the BB monomer is charged into a reactor, and AA is then added at some rate till the desired overall stoichiometric ratio is attained. It is inappropriate to use these results for the more *general*, *reversible* kinetic scheme of Table 1, particularly to stage 2 polymerization where reversibility effects and side reactions are important.

Sensitivity studies were made using the computer program for the polymerization conditions:

$$[-A]_0 = [-B]_0 = 400 \text{ mol m}^{-3}$$

$$[-A']_0 = [-AB-]_0 = [-A^*B-]_0 = [-A^\#B-]_0 = 0 \text{ mol m}^{-3}$$

$$[W]_0 = 55 \text{ mol m}^{-3}$$

$$[\lambda_{AA}^k]_0 = [\lambda_{BB}^k]_0 = 200 \text{ mol m}^{-3} \; ; \; k = 0,1,2$$

$$[\lambda_{AB}^k]_0 = [\lambda_{A'A}^k]_0 = [\lambda_{A'A'}^k]_0 = [\lambda_{A'B}^k]_0 = 0 \text{ mol m}^{-3} \; ; \; k = 0,1,2$$

$$T = 27 \, ^\circ C \tag{5}$$

The several rate constants (not the Arrhenius parameters) were varied by ±30 %, one at a time to study their effects. It was found that the results are sensitive to only two parameters, k_1 and k_4. A two-parameter curve-fit was then performed [keeping all other rate constants at their guess values (Table 2)], to obtain best-fit values of k_1 and k_4 at 27 $^\circ C$. In order to carry out this 'tuning' study, the computer code for simulation was combined with a nonlinear parameter estimation program. The Box[10] complex method was adopted for this purpose.

The Box complex procedure obtains values of the parameters, $\mathbf{p}$ ($\equiv [p_1, p_2, \ldots, p_q]$), which minimize some objective function, $E(\mathbf{p})$, using a patterned-search technique. The objective function is chosen as a weighted sum-of-square errors between values predicted by the model and some (scarce) experimental data, reported in the open literature.[11] It is given by

$$E(\mathbf{p}) \equiv E(k_1, k_4) = \sum_{i=1}^{N} w_i \left(\frac{M_{n,i,expt} - M_{n,i,theor}}{M_{n,i,expt}} \right)^2$$

$$+ \sum_{i=1}^{N} w_i \left(\frac{M_{w,i,expt} - M_{w,i,theor}}{M_{w,i,expt}} \right)^2 \tag{6}$$

In the above equation, the values of M_n and M_w are those at $t=t_f$ ($\equiv 36000$ s), the final reaction time (after which almost no further reaction takes place), N is the number of experimental data points available for M_n and M_w and w_i is the weightage factor assigned to the ith data point. Superscripts, expt and theor, represent experimental and the corresponding theoretical values. The 'tuned'

rate constants are then used to generate frequency factors for k_1 and k_4, assuming that the activation energies are the same as the guess values in Table 2. These values are given in column b in Table 2. Using these parameters, results other than for M_n and M_w (required for parameter estimation, for which experimental data is available) at 27 ^{O}C are generated. The CPU time taken on a mainframe HP9000/850S supermini computer for the parameter estimation (18 iteration) was 90 s.

CHAPTER 3

RESULTS AND DISCUSSION

The Box complex program is used as described above to obtain
the best-fit values of k_1 and k_4 at $27^{\circ}C$. The computational
parameters used in this program are given in Table 8. Figures 1-4
show some of the results generated using the Box complex code for
parameter estimation {for different values of $[P_{1,AA}]_0 + [P_{1,BB}]_0$
(equimolar amounts) but with other conditions the same as in Eq.
5}. Figure 1 shows the final values (at $t_f = 36000$ s) of the
molecular weights, M_n and M_w, predicted by the model, using the
tuned parameters (Table 2, column b). These are found to compare
well with the experimental data points of Kolegov et al.[11] for
different values of the (sum of) initial monomer concentrations,
$[P_{1,AA}]_0 + [P_{1,BB}]_0$. Figure 2 shows how the error, E (see Eq.6),
decreases with iteration number, while Figures 3 and 4 show how
the two parameters, k_1 and k_4, evolve with iteration number to
their (near) optimal values. Figure 1 also shows that the optimal
parameters fit the data better than their initial guesses, which
were fairly good. It would have been better if actual experimental
points were available *as a function of time* for each of the values
of $[P_{1,AA}]_0 + [P_{1,BB}]_0$. Unfortunately, only model predictions of
these properties have been presented by Kolegov et al.[11]

After obtaining the best-fit values of the parameters, **p** [$\equiv$
k_1, k_4], these were incorporated in the simulation program and
additional results were generated for the feed conditions of Eq.
5, i.e., for $[P_{1,AA}]_0 = [P_{1,BB}]_0 = 200$ mol m^{-3}. Figure 5 shows
the build-up of the number and weight average molecular weights

41

Table 8

Data Used in Optimal Parameter Estimation

Weightage Factors in Eq. 6

w_1 = 1

w_2 = 2

w_3 = 4

w_4 = 8

w_5 = 16

w_6 = 32

Values of Parameters of Box[10] Complex Program

N = 2

α = 1.3

β = 10^{-3}

γ = 5

δ = 10^{-5}

Initial Value of Parameter, p

$$\underset{\sim}{p} \equiv [k_1, k_4] = [6.0, 0.04]$$

Bounds on $\underset{\sim}{p}$

$$0.0 \leq k_1 \leq 10.0$$

$$0.0 \leq k_4 \leq 1.0$$

— X —
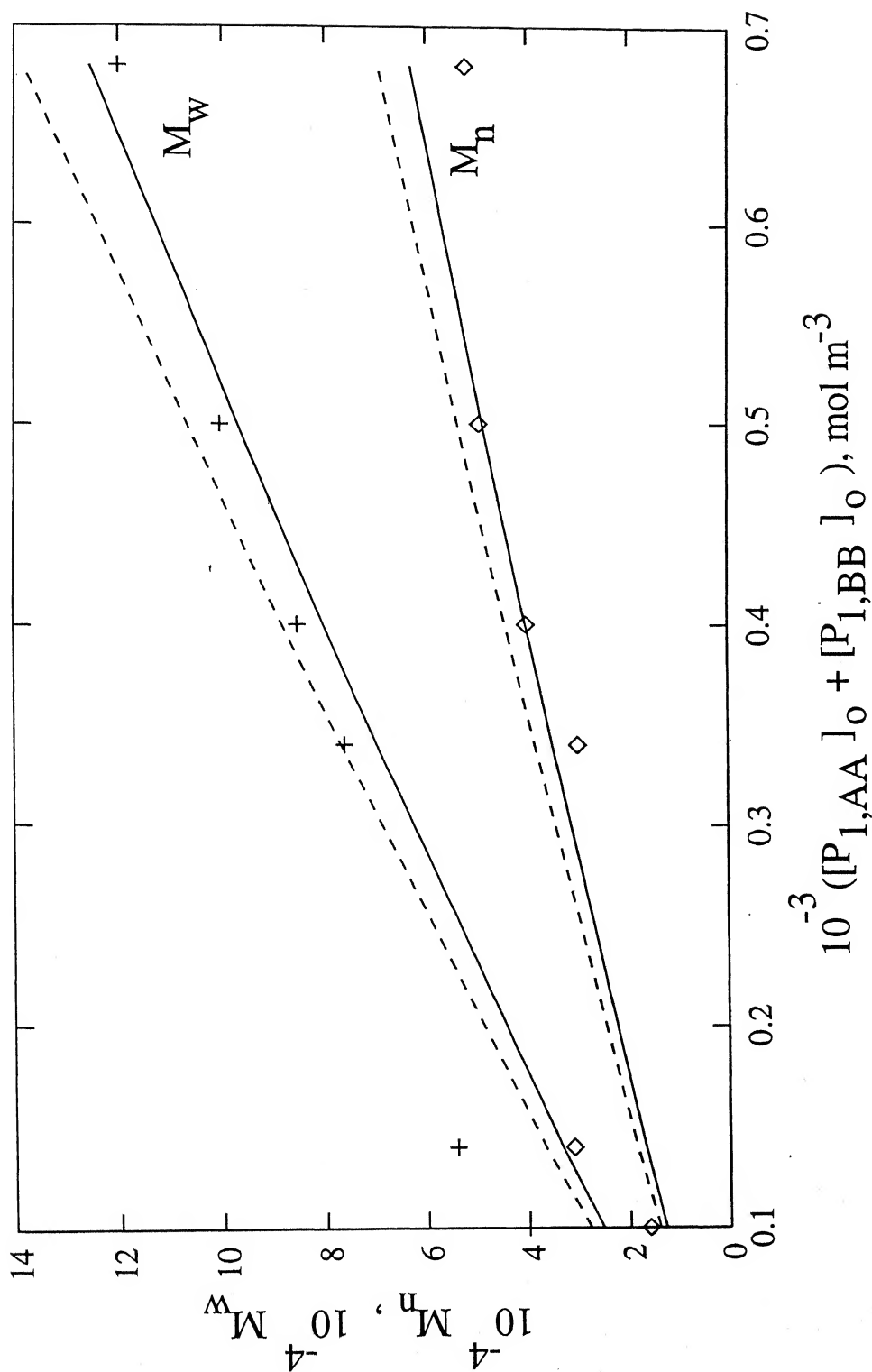
Fig. 1 Variation of molecular weights at large t_f, with the sum of initial monomer concentrations (stoichiometric amounts). Solid curves correspond to optimal parameters (Table 2 column b), while dotted curves correspond to their initial values (Table 2 column a). Experimental data points (at 27 °C) of Kolegov et al.[11] also shown.
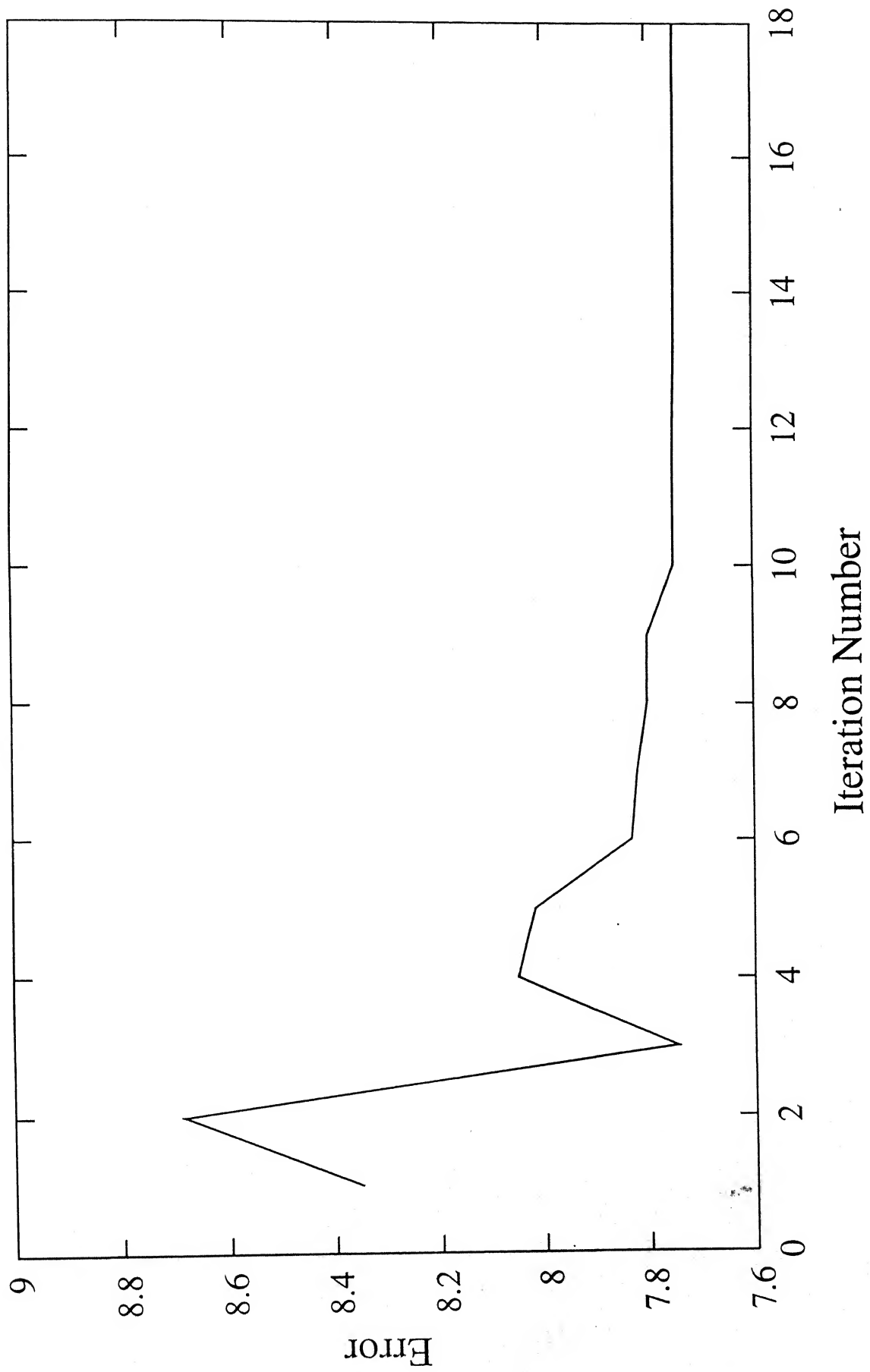
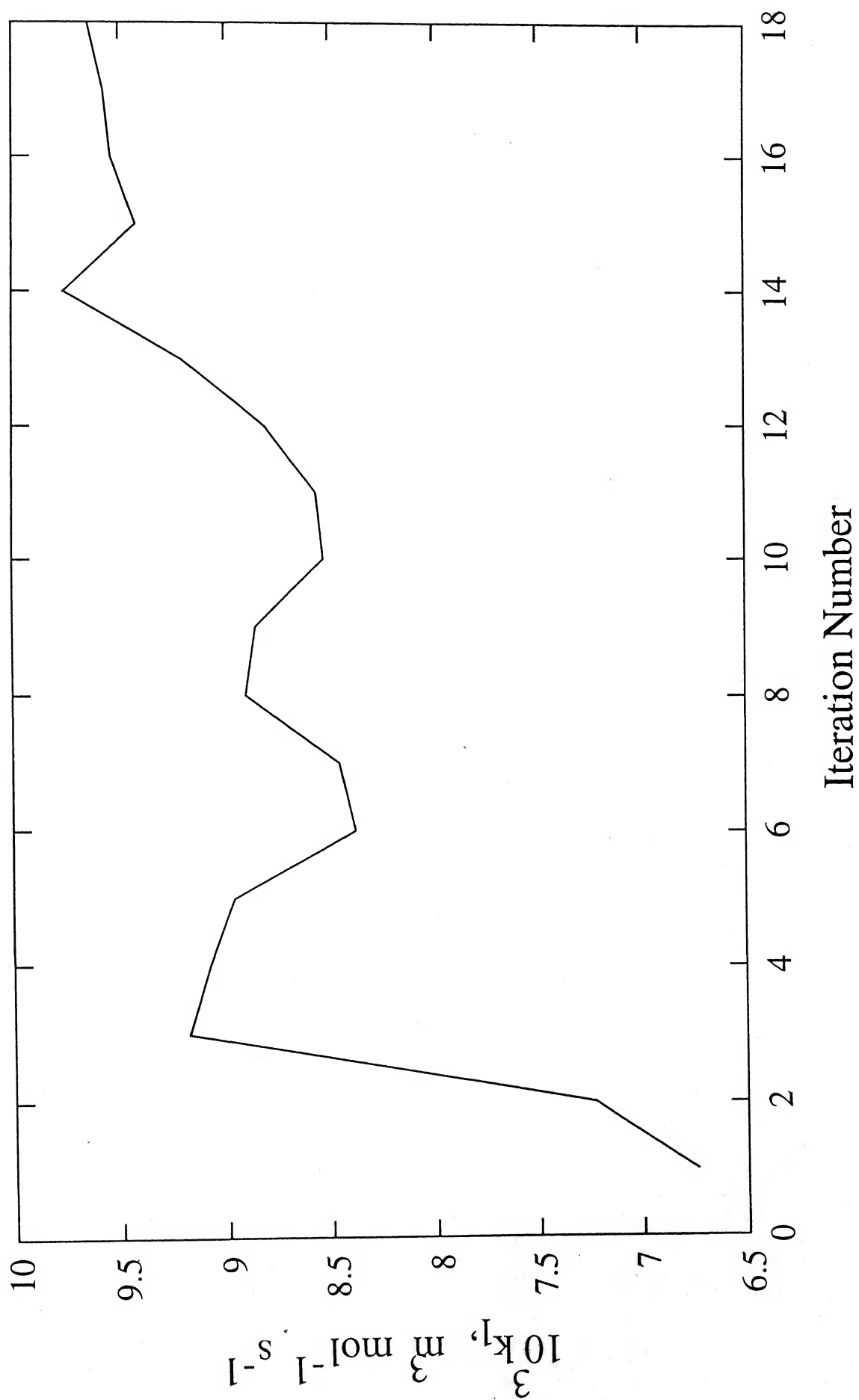Fig. 2   Variation of the error *vs.* iteration number.
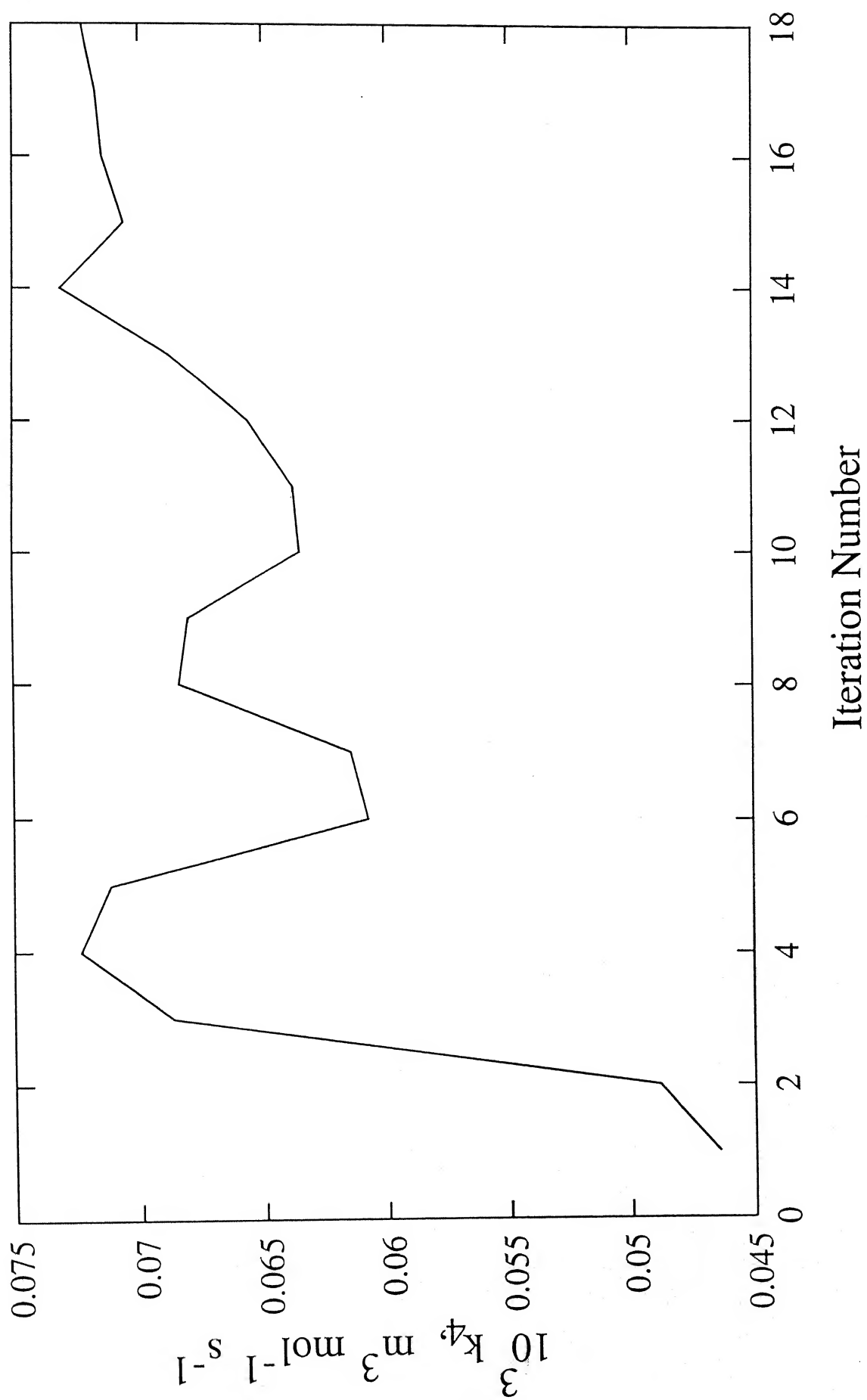
Fig. 3 Variation of k_1 with iteration number.

Fig. 4   Variation of k_4 with iteration number.

The y-axis is labelled $10^3 k_4$, m^3 mol^{-1} s^{-1} and the x-axis is labelled Iteration Number.
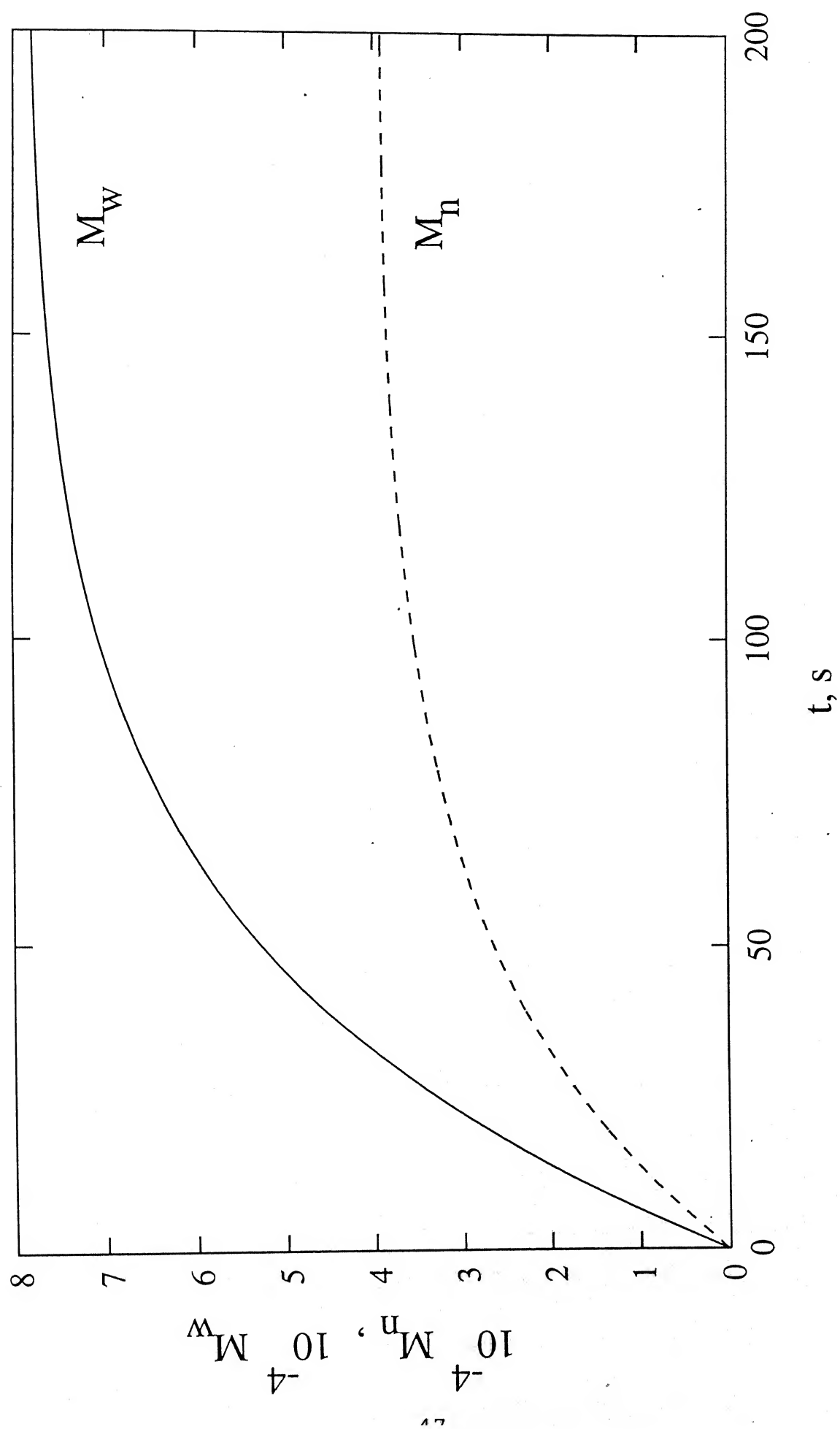
Fig. 5   Build-up of average molecular weights with time for reference conditions (feed conditions in Eq. 5, and

with time. These curves show the typical characteristics of a *reversible* polycondensation reaction in which the molecular weights reach an equilibrium value after some time. This kind of asymptotic behavior was also observed for other values of $[P_{1,AA}]_0 + [P_{1,BB}]_0$ studied in Fig. 1. Similar qualitative behaviors have been predicted by Kolegov et al.[11] under similar conditions.

The effect of the two rate constants, k_1 and k_4, on M_n and M_w are shown in Figures 6 and 7. These figures show clearly that M_n and M_w are quite sensitive to these two parameters, but that the polydispersity index, PDI, is very close to 2.0, as shown for the reference conditions (optimal values of k_1 and k_4 and feed conditions of Eq. 5) in Fig. 8 (the effect of k_1 and k_4 on PDI is minimal). Other parameters have been found to have no significant effect on M_n and M_w. Increasing k_1 while keeping k_1' unchanged speeds up the first reaction as expected, and also leads to higher molecular weight product at equilibrium due to increase in the value of its equilibrium constant. A more interesting observation is that the molecular weights decrease as k_4 is increased. This is because the increased hydrolysis of the anhydride groups at the ends of the chains to form -A′ associated with higher k_4, leads to a depletion of -A groups and this suppresses the chain lengthening process associated with the first reaction (-A′ does not participate in any chain lengthening reaction since the third reaction is irreversible, as shown in Table 1). The lack of sensitivity of results to the rate constants associated with the other reactions is because they are relatively unimportant at 27°C, the usual temperatures of polymerization in the first stage
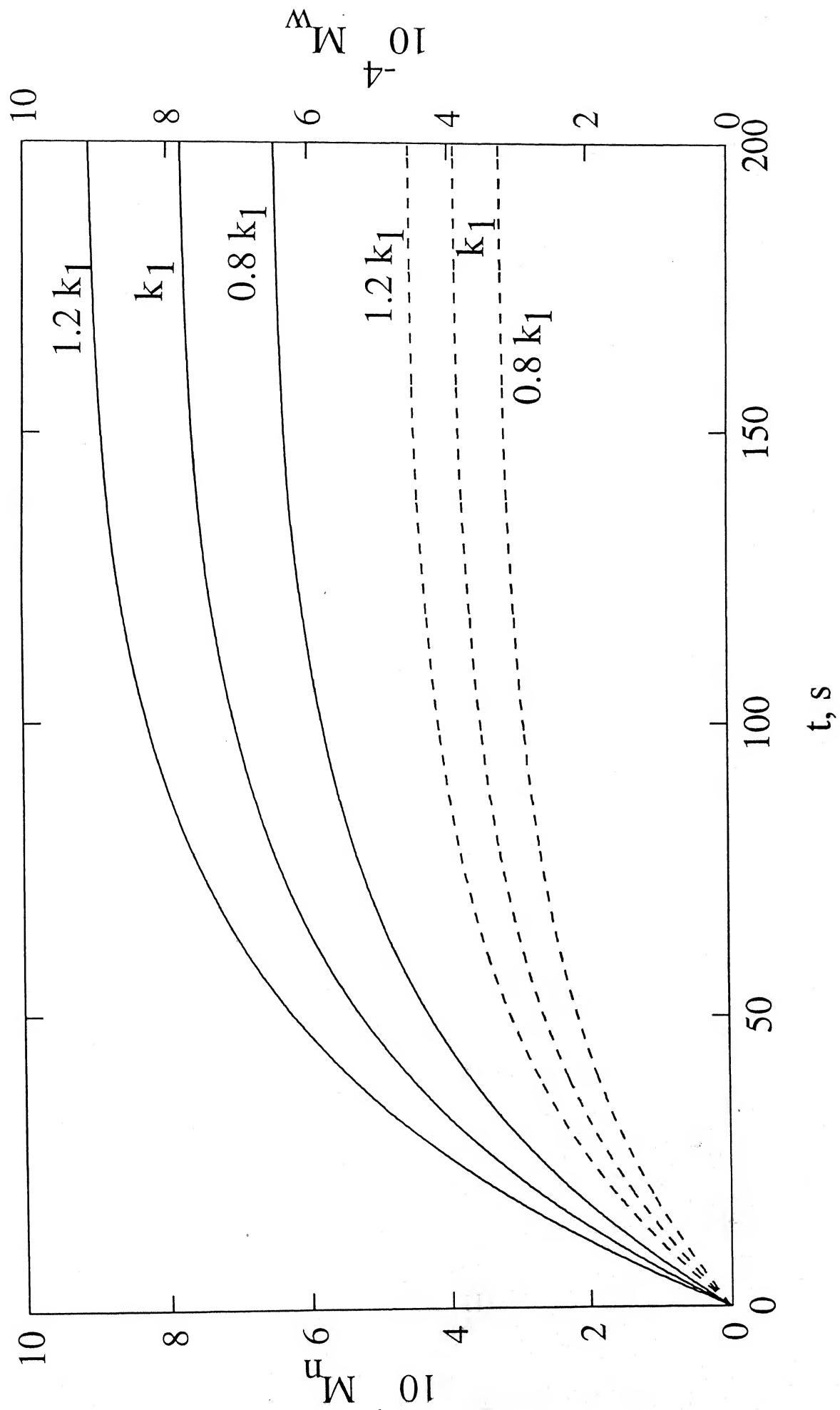
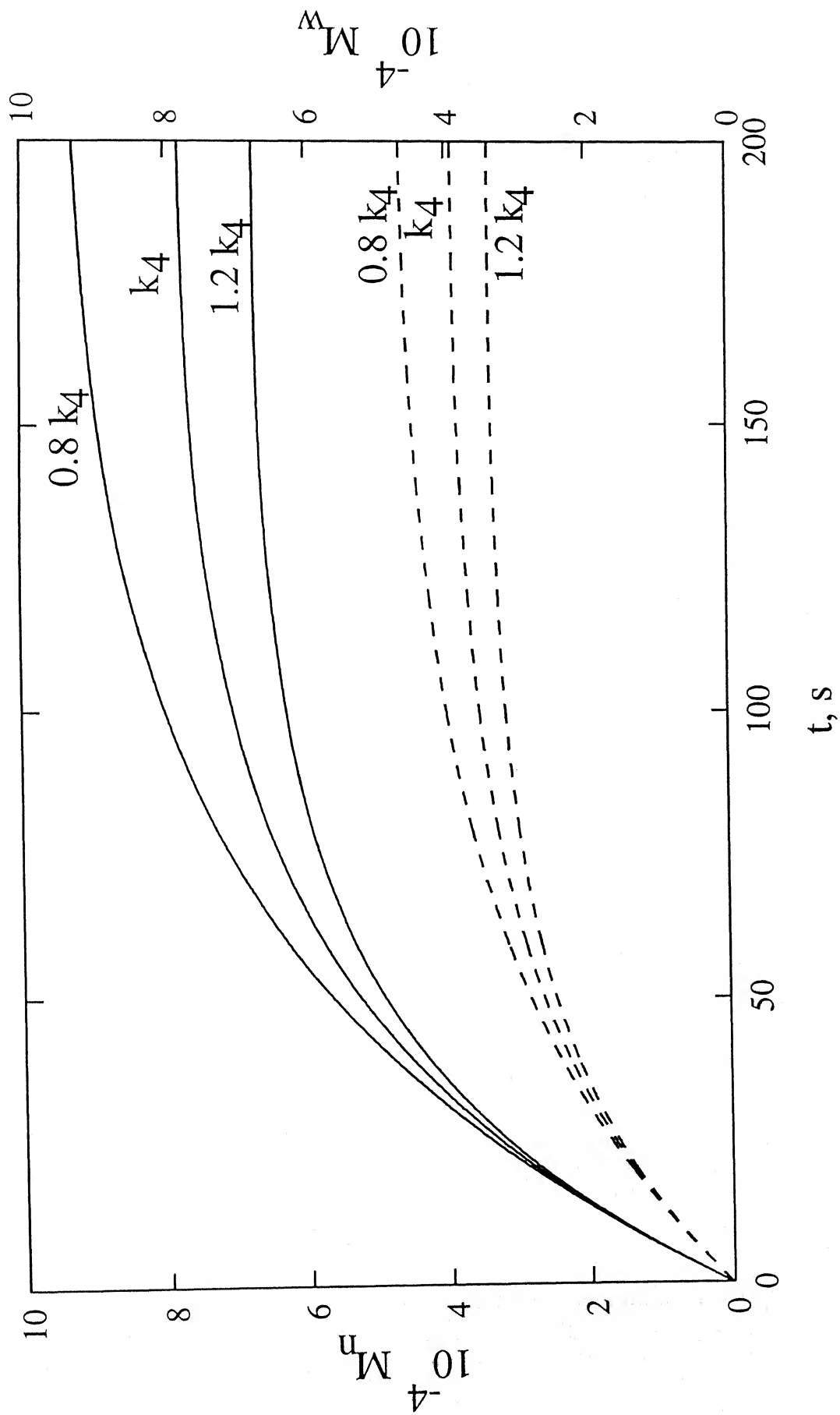Fig. 6 Effect of varying k_1 on M_n (dotted) and M_w (solid).

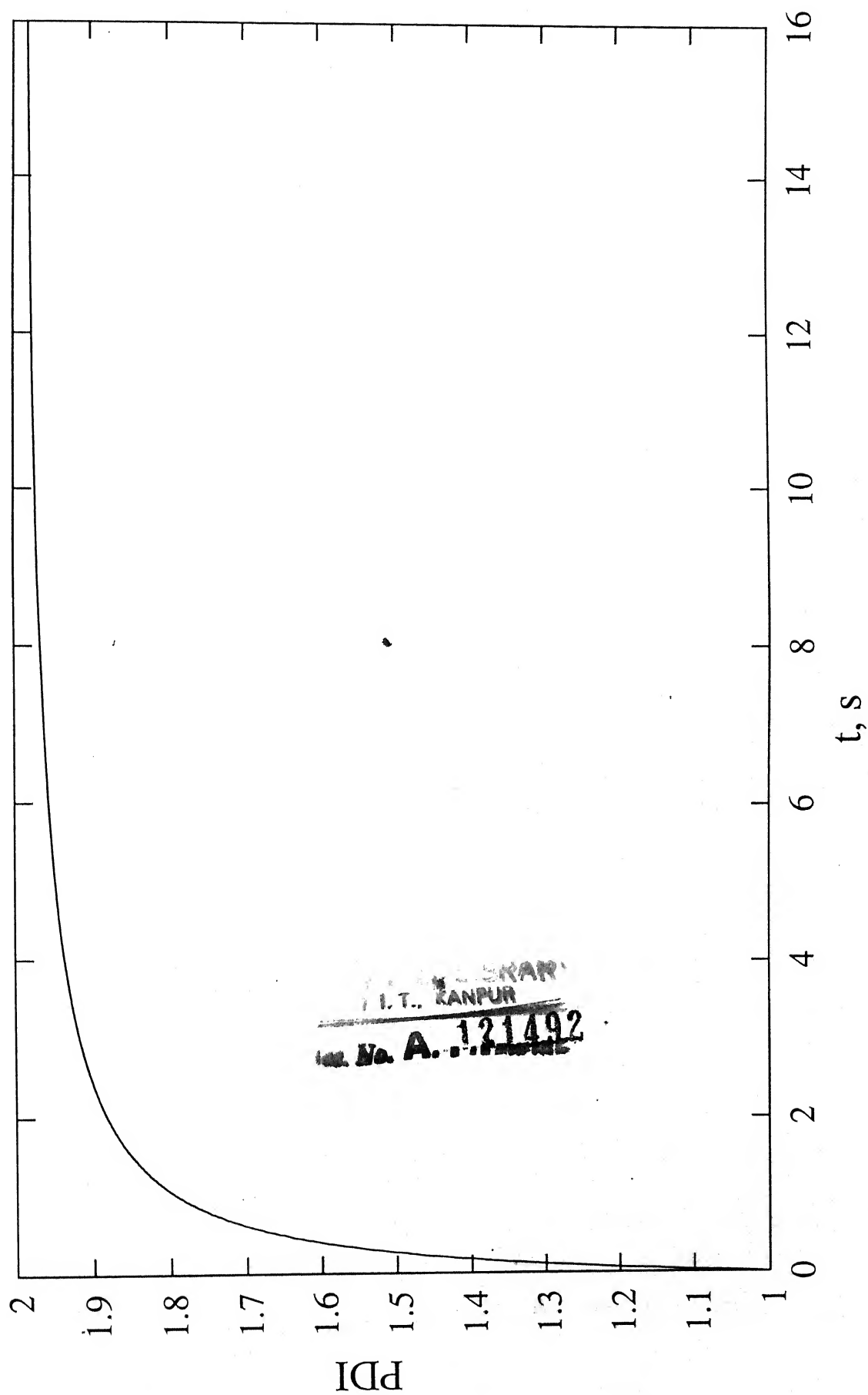Fig. 7   Effect of varying k_4 on M_n (dotted) and M_w (solid).

Fig. 8   Variation of PDI with time for the reference conditions.

51

reactor being studied. It is expected that at higher temperatures (around 130 $^\circ$C typically encountered in stage 2 reactors), the other reactions would play a more important role, and the results *may* be sensitive to variations in the associated rate constants. It is clear that these rate constants should be 'tuned' against experimental data taken on second stage reactors whenever they become available in the open literature. Till that time the general mathematical framework developed here remains un-tuned for the second stage reactors, and can be used only to provide qualitative trends (as done later in this paper).

Figure 9 shows the conversion of the monomer, $P_{1,AA}$, with time under reference conditions. It is found that the conversion of the other monomer, $P_{1,BB}$, is almost indistinguishable from that of $P_{1,AA}$, indicating that the fourth reaction in Table 1 (which depletes -A groups but not -B groups) does not contribute significantly to monomer consumption in the first 4 seconds in which most of the monomers are consumed. The rapid depletion of monomer is typical of step growth polymerizations.[9] It may be emphasized that the fourth reaction does, indeed, affect the molecular weight at later times (this explains the decrease in M_n and M_w as k_4 increases, in Figure 7), which is associated with an increase in [-A'] with t (see Figure 10). The concentration of -A functional groups decreases at a slightly slower rate than $[P_{1,AA}]$.

The average molecular weights of PAA can be controlled by varying the stoichiometric ratio, $R \equiv [P_{1,AA}]_0 / [P_{1,BB}]_0$. A small variation in R away from unity results in a significant drop in the molecular weight, as shown in Figure 11. This behavior is
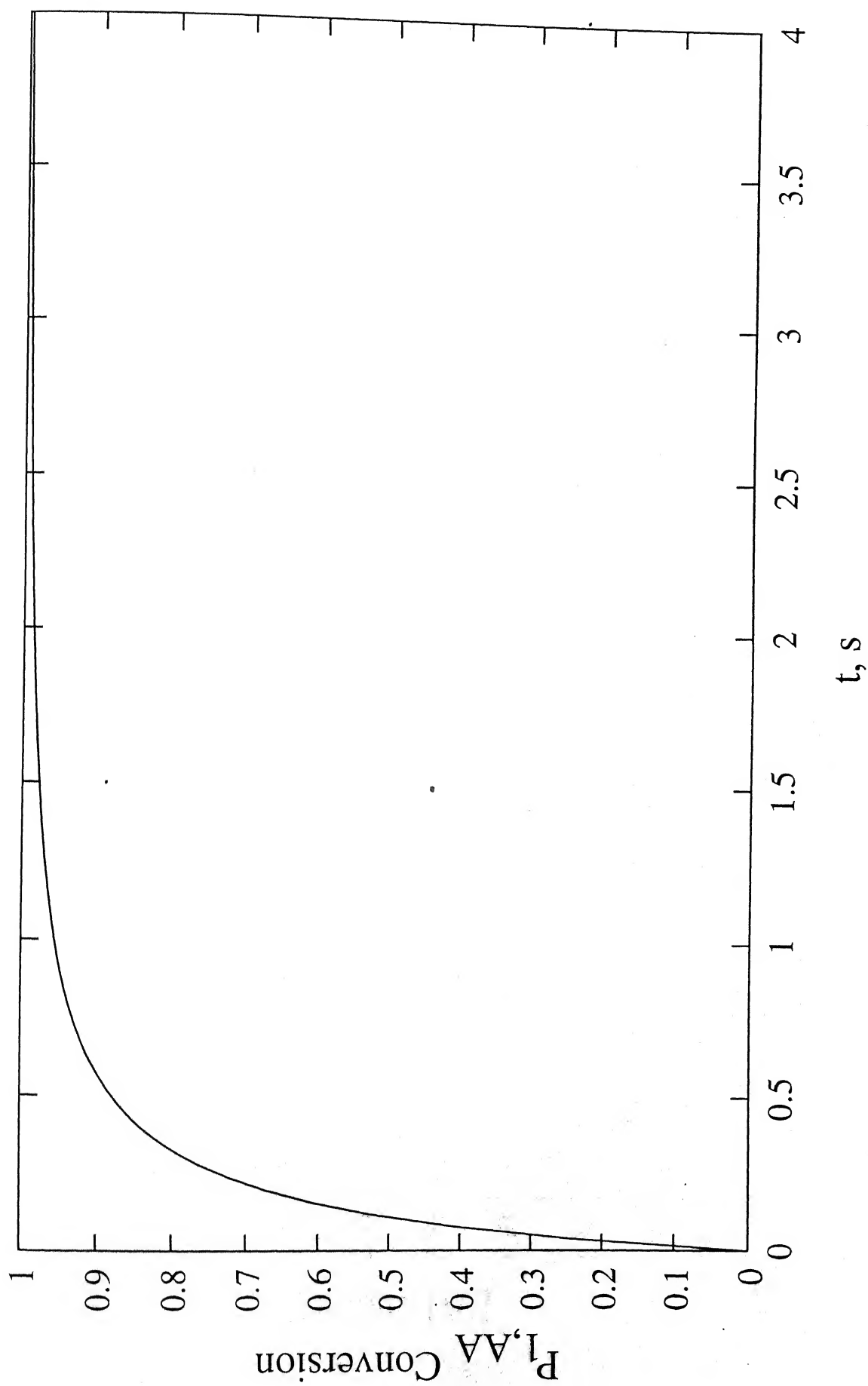
Fig. 9   Variation of the conversion of $P_{1,AA}$ with time for the reference conditions.
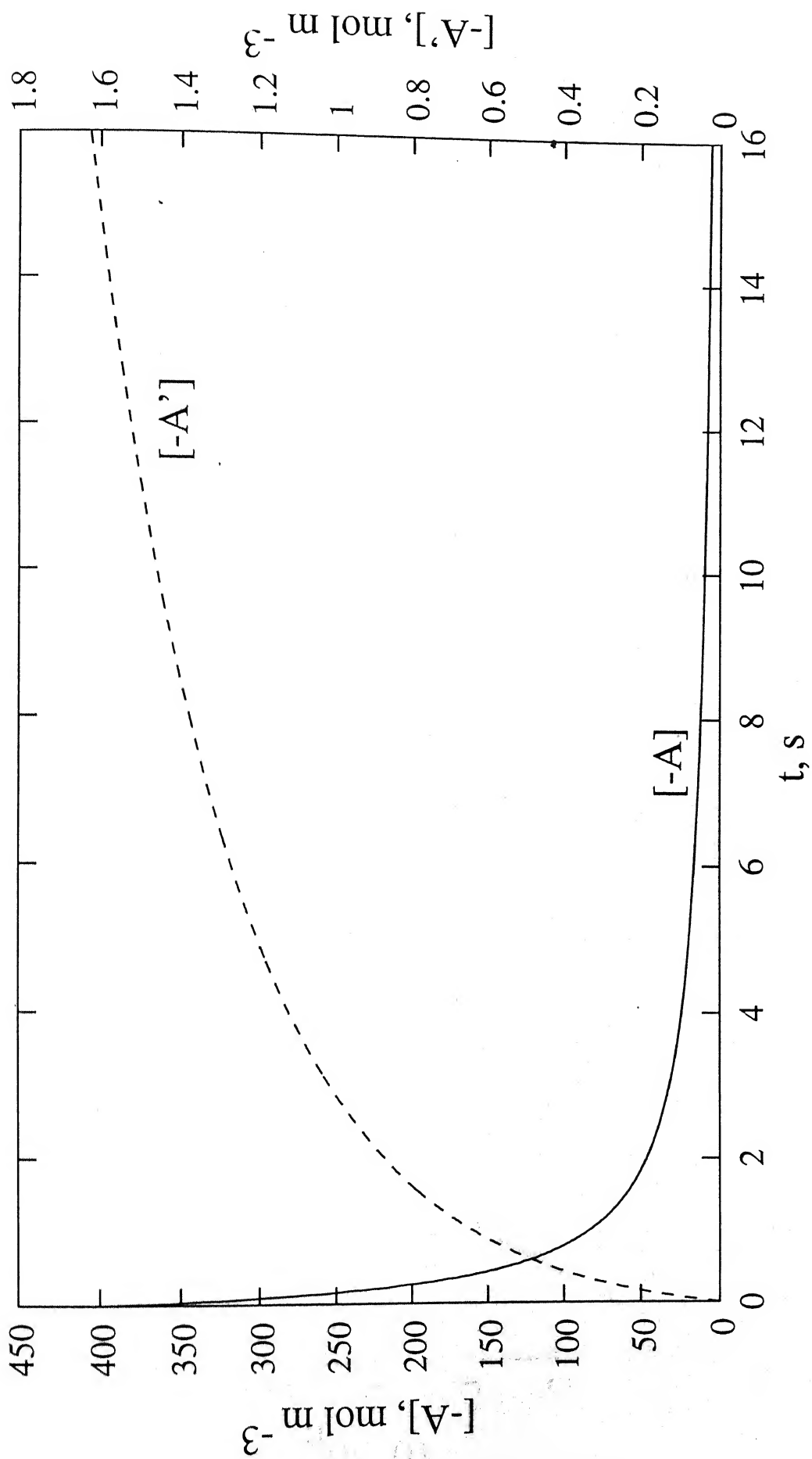
Fig. 10   Conversion of -A (or -B) and -A' functional end groups for
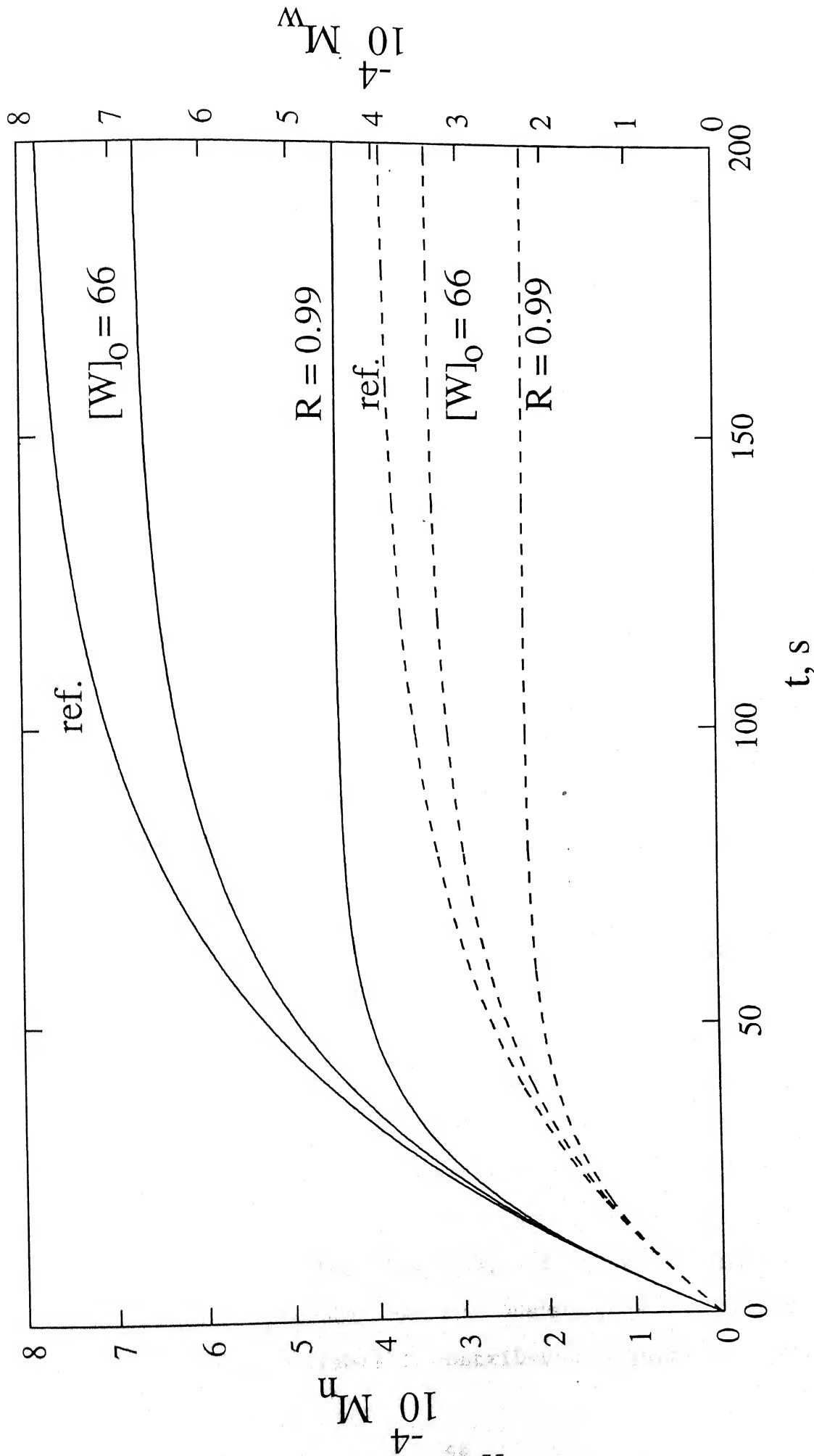the reference conditions.

Fig. 11 Effect of stoichiometric ratio, $R \equiv [P_{1,AA}]_0 / [P_{1,BB}]_0$ and of $[W]_0$ on M_n (dotted) and M_w (solid). Curves for the reference conditions ($R = 1.0$, $[W]_0 = 55$ mol m^{-3}) also

similar to that exhibited by (irreversible) AA + BB step growth polymerizations,[9] which is not surprising since Rxn. 1 in Table 1 is the main reaction under reference conditions. Again, the PDI attains a value of 2.0 quite early. The reaction (in stage 1) is also quite sensitive to the initial water concentration.[11] Figure 11 shows how the average molecular weight changes when $[W]_0$ is increased from the reference value of 55 to 66.0 mol m^{-3} (1.2 times the reference value). The importance of proper metering of the monomers and control of their purity is brought out by this diagram. Figure 12 shows how the fraction of imide links and of the unfavoured conformer, f_{A^*B} and $f_{A^\#B}$ respectively, vary with time. Both these fractions are negligible at reference (first stage) conditions, and f_{AB} rises very rapidly to a value near unity. This confirms that Rxns. 2 and 5 are relatively unimportant at low temperatures. The variation of the acid group concentration, [-COOH], with time is shown in Figure 13. These can be experimentally measured by titration. The increase in [-COOH] with time compares qualitatively with the experimental results of Johnson[7] on a different system (his equivalent weights are evaluated such that they show the opposite trends than shown by [-COOH]).

The moment closure approximations (Table 6) were changed by incorporating a multiplying factor on the right hand side of the equations. No significant differences were found in *all* the results at 27 °C when a factor of 1.2 (or larger) was used. This insensitivity of results justifies the use of these closure conditions and is probably because under these conditions, only the first reaction in Table 1 contributes significantly (and the
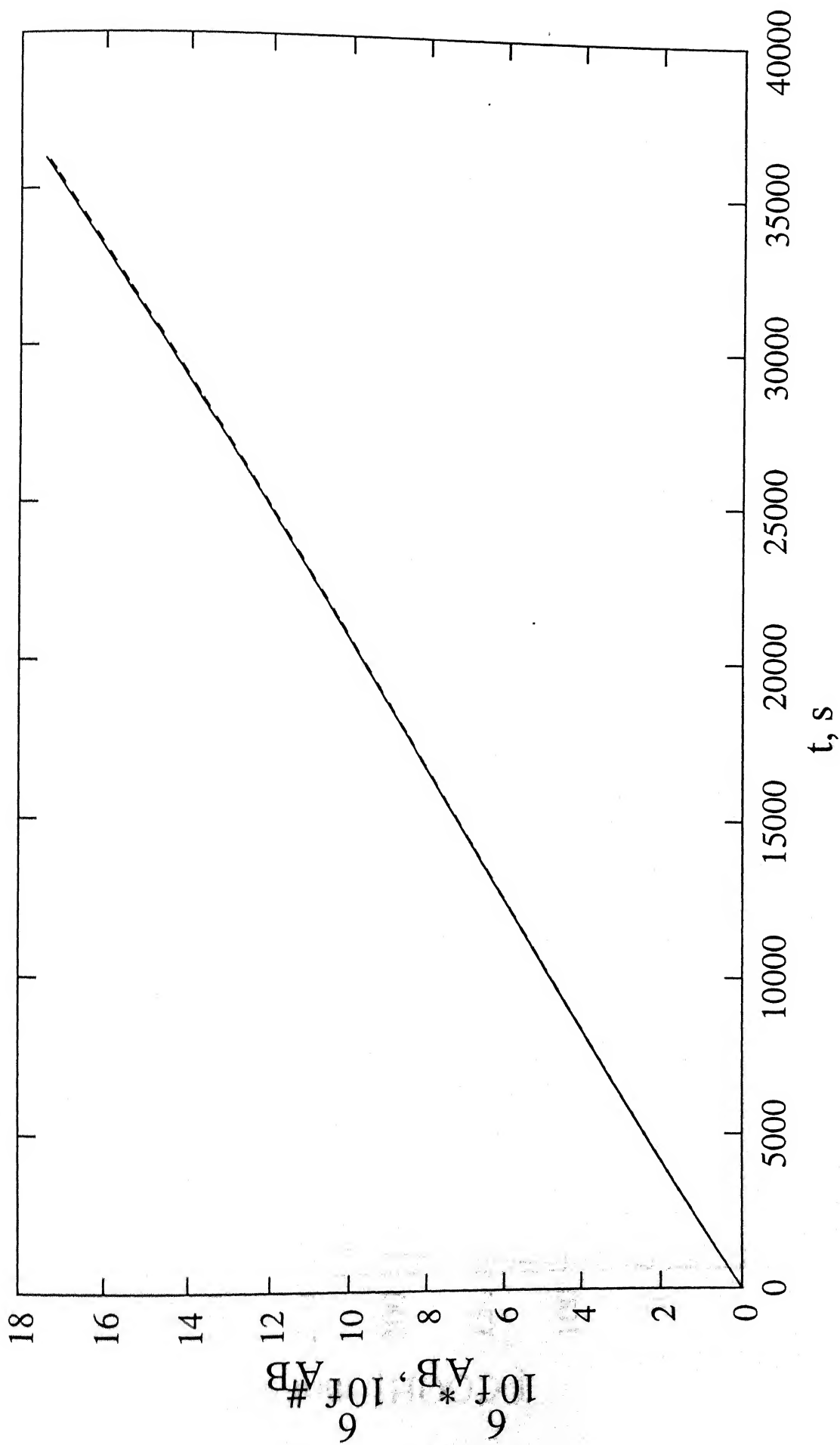
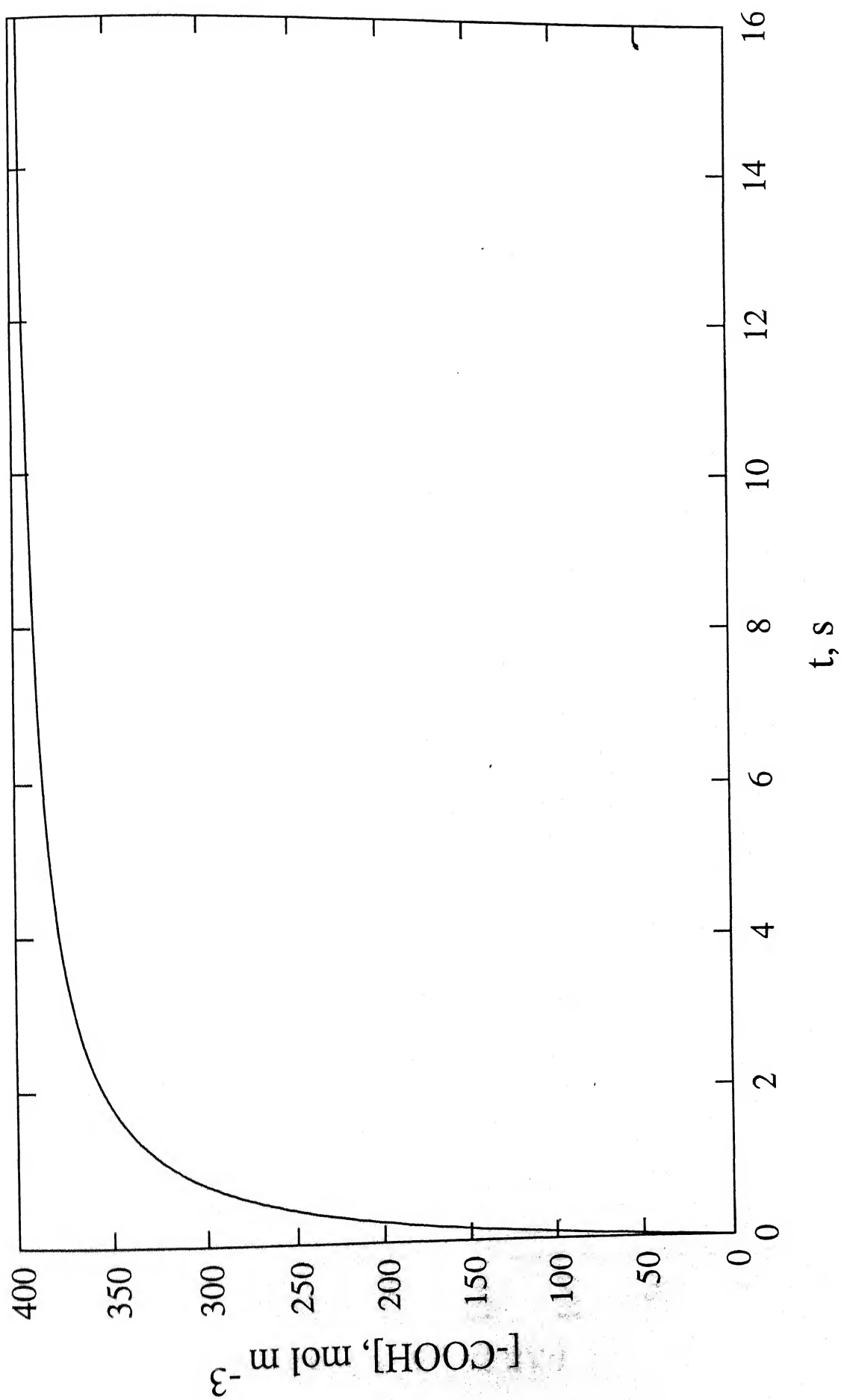Fig. 12 Variation of the fractions, f_A*_B (solid) and $f_A\#_B$ (dotted), with time for the reference conditions.

57

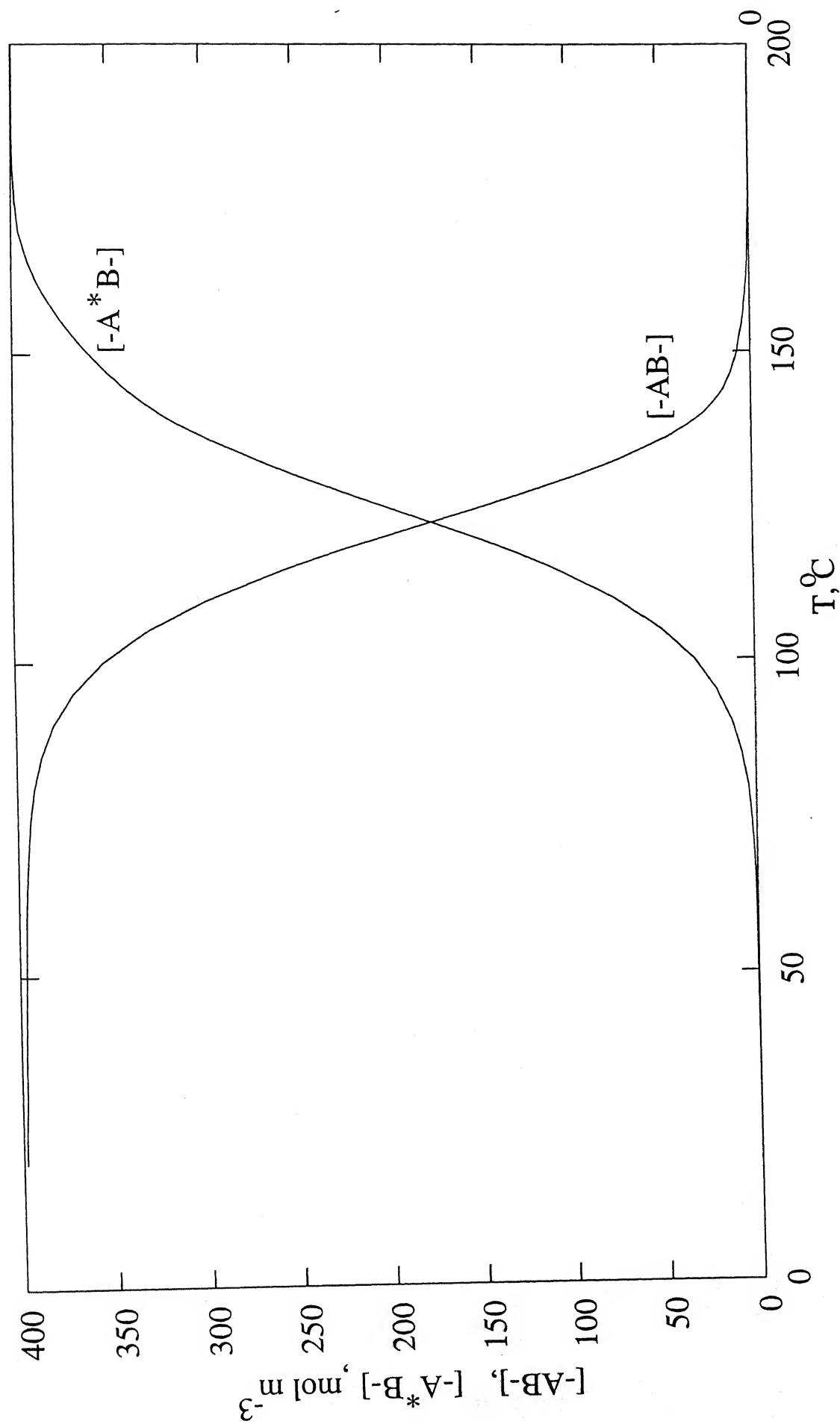Fig. 13 Variation of [-COOH] with time for the reference conditions.

Fig. 14   Concentrations of -A*B- and -AB- at large times (36000 s) for the reference conditions (but with T different than in
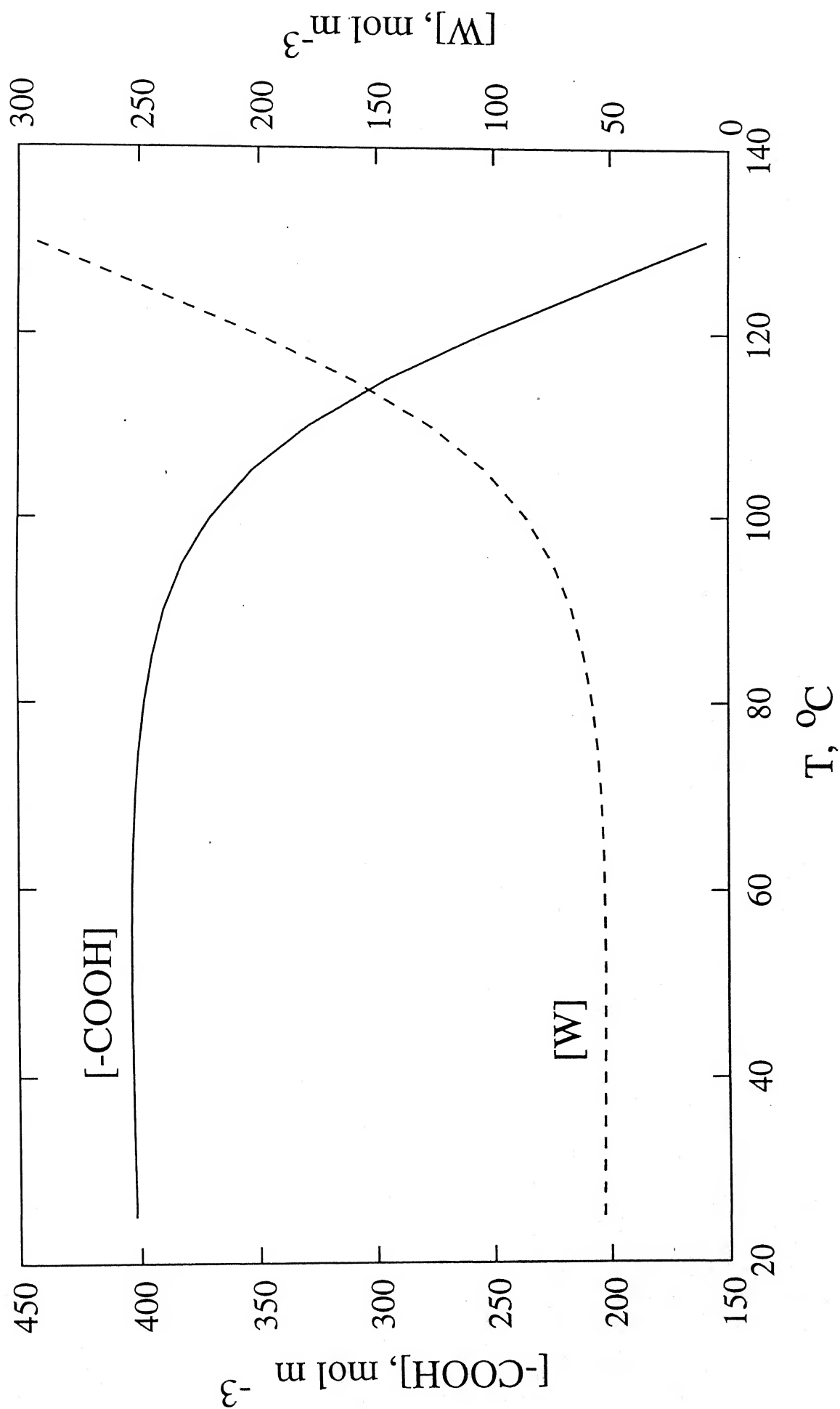
Fig. 15 [-COOH] and [W] at large times (36000 s) for the reference
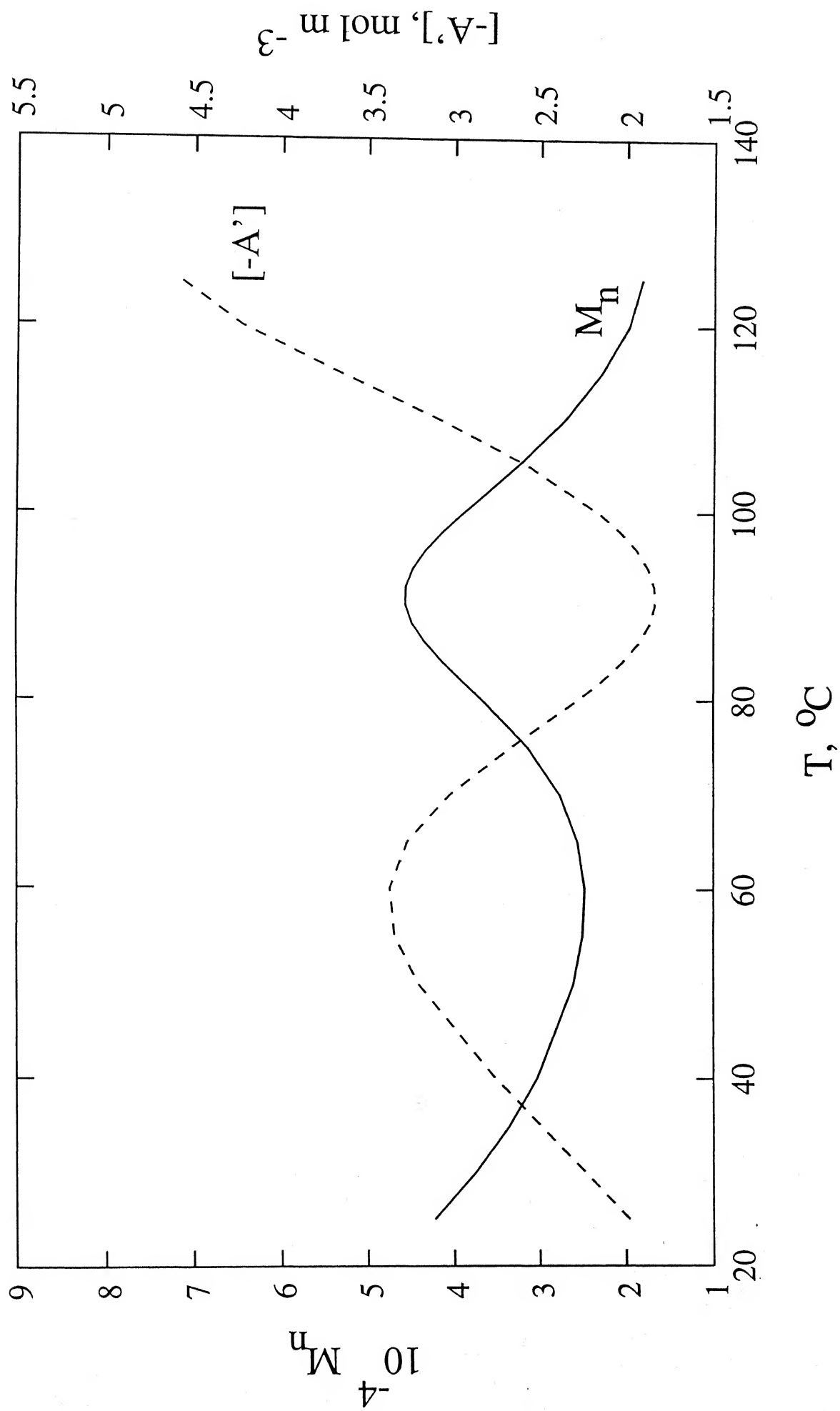conditions (but with T different than in Eq. 5).

Fig. 16 M_n and $[-A']$ at t = 36000 s for the reference conditions of Eq. 5 (but with T different).
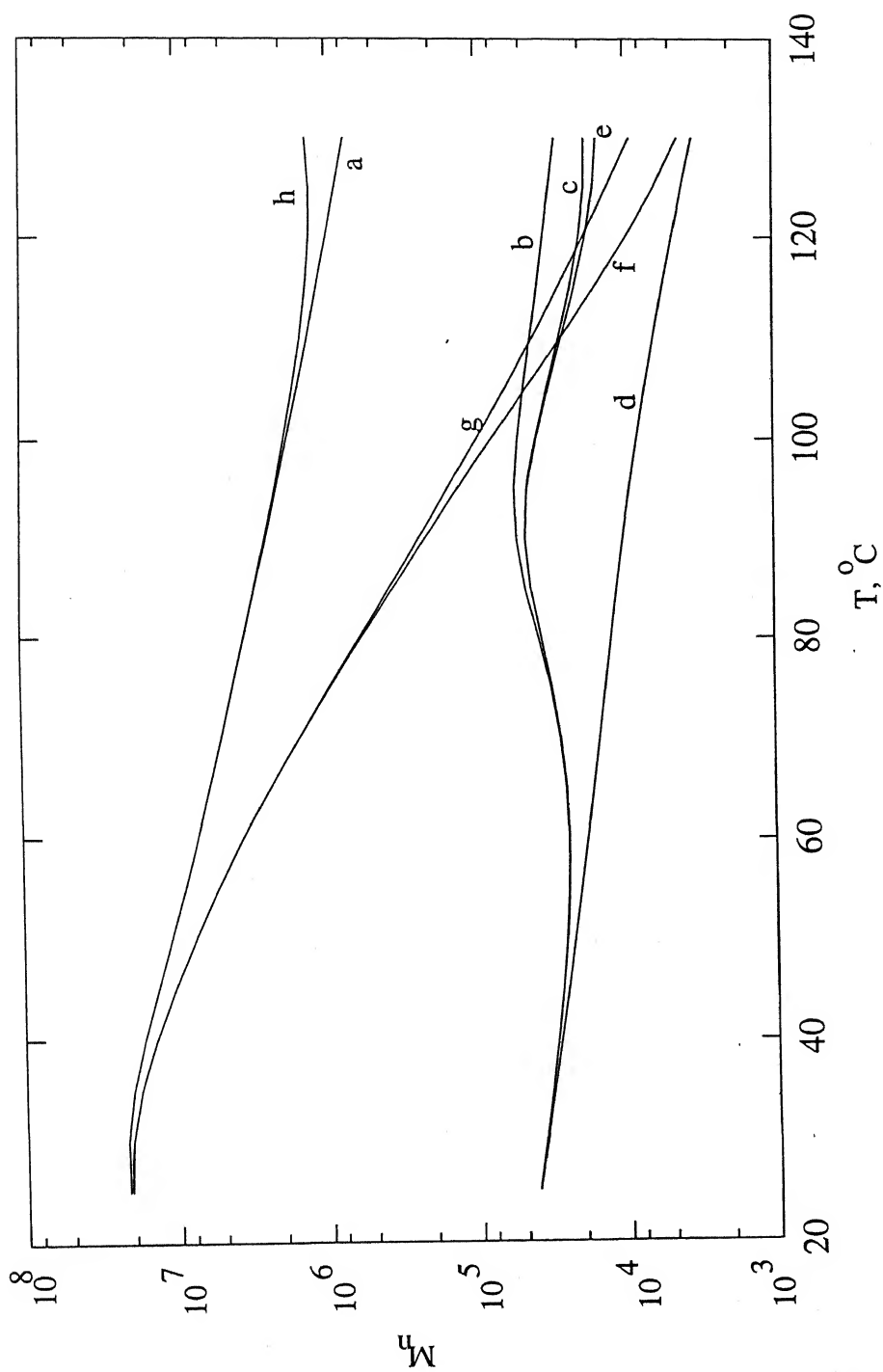
Fig. 17 M_n at t = 36000 s as a function of temperature for all or some of the reactions of Table 1. Reference conditions (except T) of Eq. 5 used. Curve a: Rxn. 1 only; Curve b: Rxns. 1, 4; Curve c: Rxns. 1-5; Curve d: k_1, k_1' and k_4 nonzero; Curve e: Rxns. 1-4; Curve f: Rxns. 1-3; Curve g: Rxns. 1, 3; Curve h: Rxns. 1, 2.

closure conditions have been well tested for this reaction[9]).

Figures 14-16 show how the values of $[-A^*B-]$, $[-AB-]$, $[-COOH]$ and M_n at large values of t (= 36000 s), vary with temperature. The initial conditions are the same as given in Eq. 5. Again, Johnson[7] has provided *some* experimental results similar to these (for PAA prepared from a different diamine). Figure 14 shows that much higher concentrations of imide links are attained at higher temperatures, at the cost of the amide links (-AB-). Such a phenomenon has been predicted *qualitatively* by Johnson,[7] and reflects the importance of Rxn. 2 in Table 1 at high temperatures. Figure 15 shows that the concentration of acid groups decreases at high temperatures as they get consumed by the imidization reaction. This is exactly opposite to the trend shown by the equivalent weight *vs*. T plot of Johnson.[7]

Figure 16 shows how M_n at high values of t (= 36000 s) varies with temperature. This diagram also shows how an increase (or decrease) in M_n is associated with a simultaneous decrease (or increase) of the concentration of -A'. Figure 17 shows M_n (at t = 36000 s) *vs*. T for several combinations of the reactions of Table 1. Curve a shows the results when *only* Rxn. 1 (Table 1) is considered. Higher temperatures lead to higher values of k_1' (relative to k_1), and lead to lower chain lengths for the exothermic Rxn. 1. Just by adding on Rxn. 4 to this reaction, we find (curve b) that the value of M_n is reduced by almost three orders of magnitude. This is because Rxn. 4 depletes the -A end groups (converting them to -A') and thus reduces the chain growth process of Rxn. 1. It is obvious (see curves b and c) that Rxns. 2, 3 and 5 do not contribute significantly till about 80 $^\circ$C. The

decrease of M_n followed by an increase and then, again, a decrease, as T increases from about 25°C to 90°C is, clearly, due to the effect of Rxn. 4 on Rxn. 1 (see curve b). The reverse step of Rxn. 4 dominates in 60°C ≤ T≤ 90°C while the reverse step of Rxn. 1 dominates for T > 90 °C. In fact, the local minima/maxima is not observed if only k_1, k_1' and k_4 are nonzero (see curves a, b and d). At T > 90 °C, Rxns. 2, 3 and 5 also affect M_n (see curves b, c and e). W produced by Rxn. 2 leads to chain scission through Rxn. 3, thus giving lower molecular weight product. It may be mentioned that Johnson[7] has found that the viscosity of polymer formed at large values of t decreases as the temperature increases. However, he does not study very high temperatures and so it is not too clear if the behavior shown in Figure 17 is indeed observed experimentally. If detailed experiments become available, one can 'tune' the rate constants associated with Rxns. 2, 3 and 5 and get better predictions.

Figures 18-20 show some results for simulating the second stage (curing) operation (earlier results were for the first stage at different T). The initial conditions for generating these results are the same as at the end of stage 1 (t = 36000 s in stage 1, at 27°C):

Stage 2

at t=0:

$$[-A]_0 = 0.47 \times 10^{-4} \text{ mol m}^{-3} ; \quad [-AB-]_0 = 0.40 \times 10^{+3} \text{ mol m}^{-3}$$

$$[-A']_0 = 0.21 \times 10^{+1} \text{ mol m}^{-3} ; \quad [-A^*B-]_0 = 0.69 \times 10^{-2} \text{ mol m}^{-3}$$

$$[-B]_0 = 0.21 \times 10^{+1} \text{ mol m}^{-3} ; \quad [-A^\#B-]_0 = 0.69 \times 10^{-2} \text{ mol m}^{-3}$$

$$[W]_0 = 0.53 \times 10^{+2} \text{ mol m}^{-3}$$

(7)

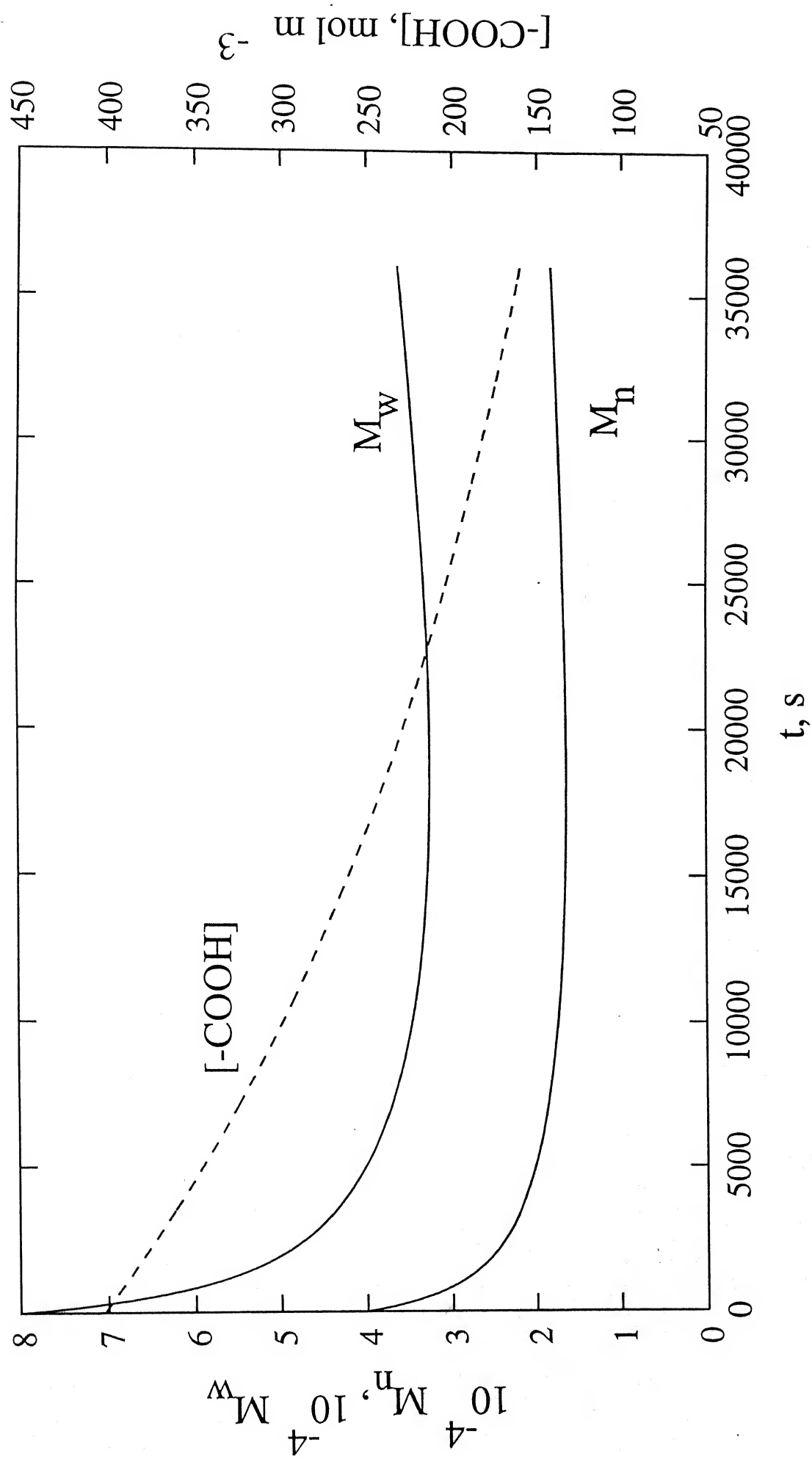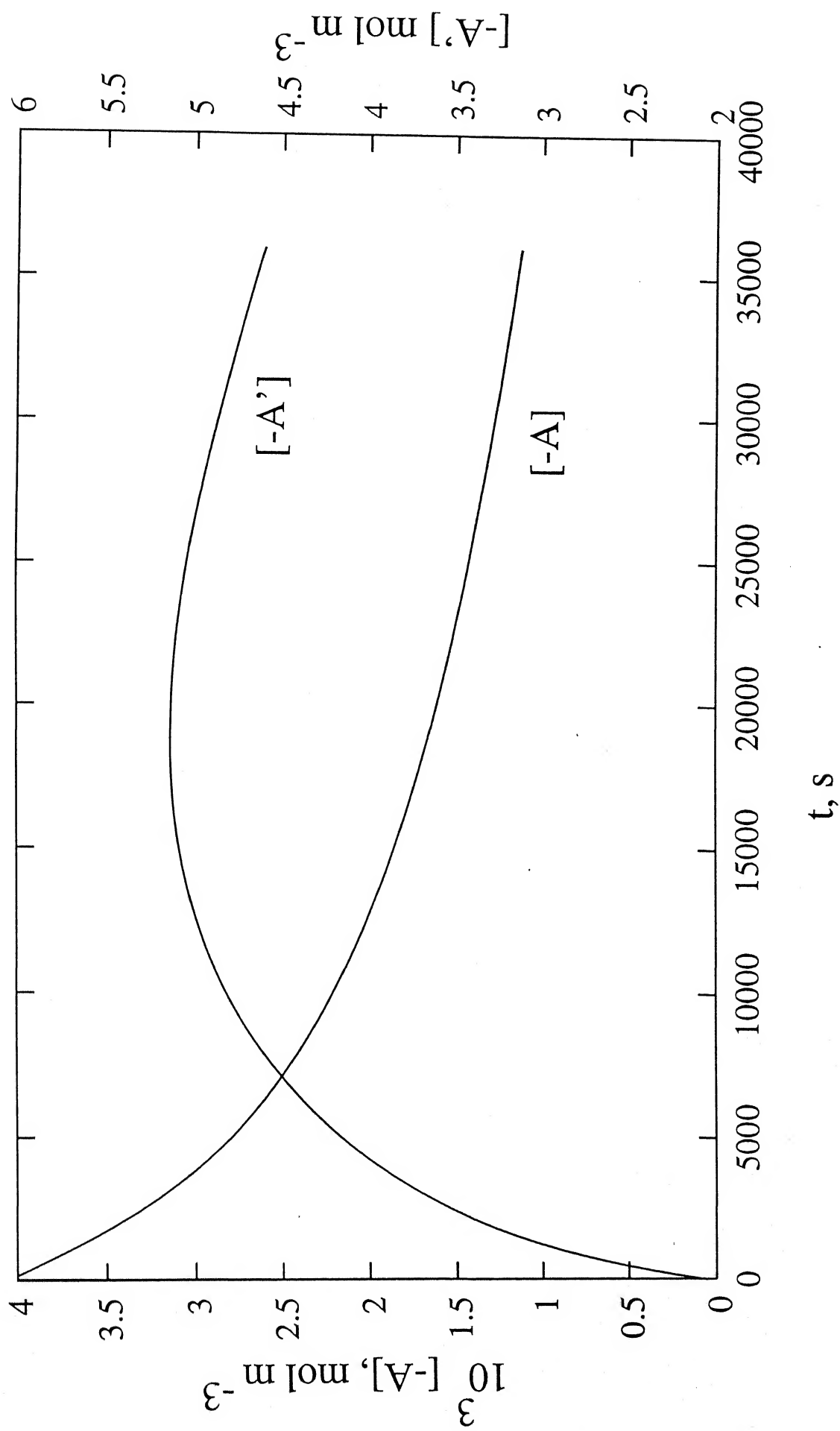Fig. 18 Variation of M_n, M_w and [-COOH] with time for stage 2 polymerization.

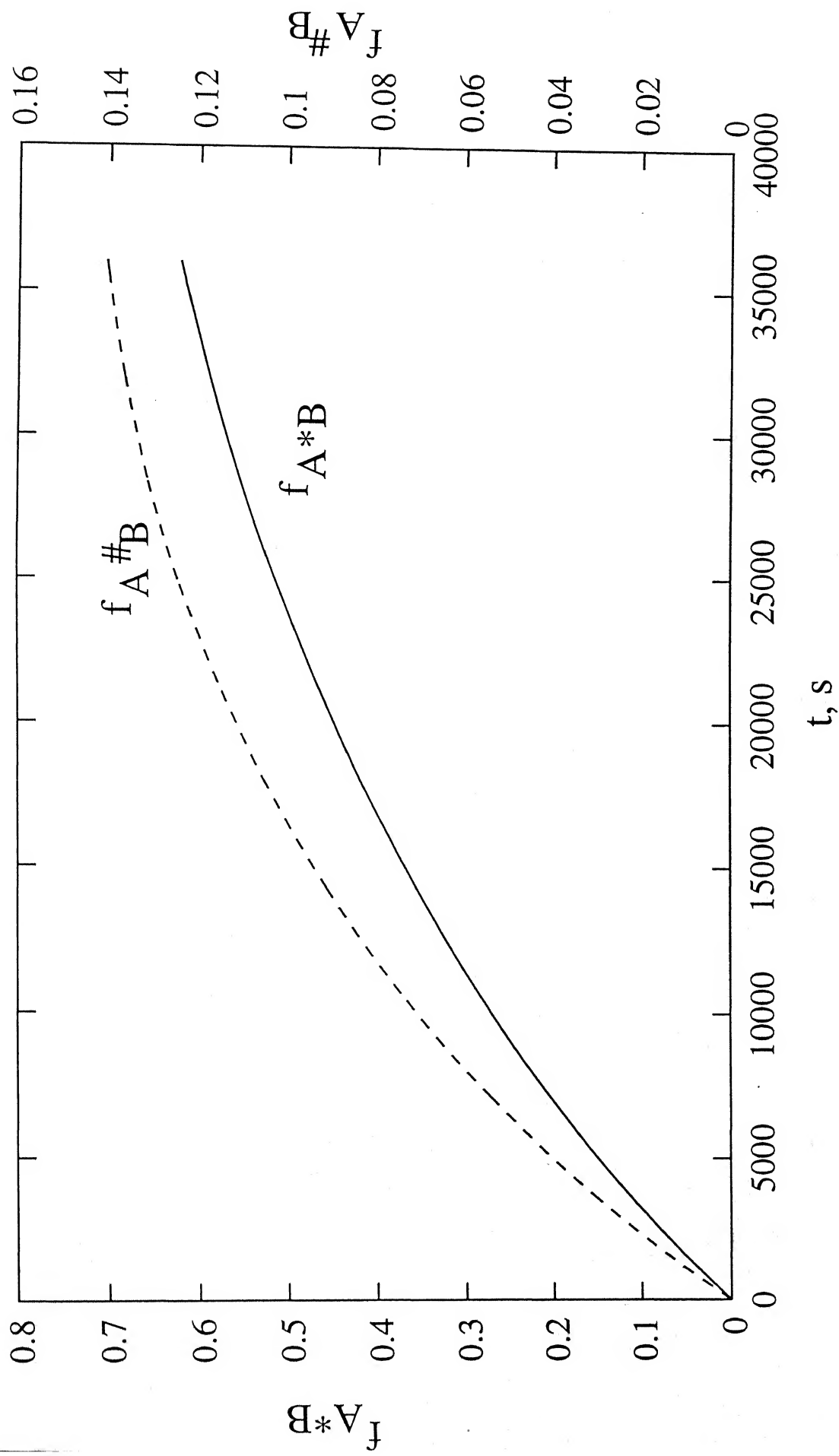Fig. 19 Variation of [-A] and [-A'] with time for stage 2 polymerization.

Fig. 20 Variation of f_{A*B} and $f_{A\#B}$ with time for stage 2 polymerization.

Other values (moments) can be supplied on request. The temperature is selected as 130 $^{\circ}$C (isothermal). It is assumed that the solvent is not removed at the end of stage 1 (i.e., a film is *not* cast and *then* cured). Since little experimental data is available for the curing of PAA films against which our results can be tested (or tuned), and since the objective of generating these results is *solely* to test whether our model can, indeed, predict some important qualitative features expected in stage 2, removal of the solvent before curing was not effected. Indeed, several additional physico-chemical phenomena (e.g., removal of water through the solid film, dependence of rate constants on the 'viscosity' of the film, heat transfer across the solid film, etc.) need to be accounted for simultaneously in the present *kinetic* model before curing of PAA *films* at high temperatures can really be modeled.

Figure 18 shows how M_n and M_w decrease with time (due to the chain scission reaction). However, these increase *slightly* after about t = 20000 s. This is associated with a simultaneous increase in -A' concentration, as shown in Figure 19. The continuous increase of $f_A{}^*{}_B$ and $f_A{}^\#{}_B$ with time for the same situation is shown in Figure 20. It is clear from Table 1 that the reverse step of Rxn. 4 starts playing an important role at high values of t, and converts -A' to -A (relatively speaking), thus leading to higher M_n and M_w (through Rxn. 1) as well as lower [-A'] at large times. The importance of the reverse step of Rxn. 4 in Table 1, is to be noted. It has also been found that the molecular weights are relatively insensitive to variations of k_2, k_3' and [W]$_0$ in stage 2.

The effect of introducing a multiplying factor of 1.2 on the

right hand sides of *all* the moment closure equations in Table 6, was also studied. The value of M_w (at t = 36000 s) decreased by less than a few percent by using this factor in all the closure equations simultaneously. The difference was quite small if only one closure equation was modified at a time. This suggests that these closure equations can possibly be used for the second stage reactor. However, the sensitivity of results to the moment closure equations needs to be studied again after tuning the rate constants for Rxns. 2, 3 and 4 on experimental data for the curing process.

CHAPTER 4

CONCLUSIONS

A comprehensive kinetic model has been presented in this study. This model can easily be adapted to account for limitations of heat and mass transfer which are normally encountered in large scale reactors. A few of the rate constants have been curve-fitted against a limited amount of experimental data available at low temperatures, from the open literature. However, detailed experimental results, particularly at high temperatures, are required so as to get 'tuned' values for the other rate constants, in particular, Rxns. 2, 3 and 5 of Table 1.

REFERENCES

1   Numata, S., Oohara, S., Imaizumi, J. and Kinjo, N., *Polym. J.*, 1985, **17**, 981

2   Numata, S., Oohara, S., Fujisaka, K., Imaizumi, J. and Kinjo, N., *J. Appl. Polym. Sci.*, 1986, **31**, 101

3   Sroog, C.E., *J. Polym. Sci.*, C, 1967, **16**, 1191

4   Sroog, C., *Encyclopedia of Polymer Science and Technology*, Vol. 11, Bikales, N.M., Mark, H.F. and Gaylord, N.G., eds., 1st ed., 1969, p.247

5   Sroog, C.E., Endrey, A.L., Abramo, S.V., Berr, C.E., Edwards, W.M. and Olivier, K.L., *J. Polym. Sci.*, A, 1965, **3**, 1373

6   Bower, G.M. and Frost, L.W., *J. Polym. Sci.*, A, 1963, **1**, 3135

7   Johnson, E.L., *J. Appl. Polym. Sci.*, 1971, **15**, 2825

8   Ray, W.H., *J. Macromol. Sci.*, *Revs. Macromol. Chem.*, 1972, **C8**, 1

9   Kumar, A. and Gupta, S.K., *Reaction Engineering of Step Growth Polymerization*, Plenum, New York, 1987

10   Box, M., *Computer J.*, 1965, **8**, 42

11   Kolegov, V.I., Belenkii, B.G. and Frenkel, S.Ya., *Vysokomol. Soyed.*, 1977, **A19**, 1873

12   Kolegov, V.I., and Frenkel, S.Ya., *Vysokomol. Soyed.*, 1976, **A18**, 1680

13   Kolegov, V.I., *Vysokomol. Soyed.*,1976, **A18**, 1689

14   Tsiang, R. C-C, and J.M. Liu, *Ind. Eng. Chem. Res.*, 1995, **34**, 4260

15   Kruez, J.A., Endrey, A.L., Gay, F.P. and Sroog, C.E., *J. Polym. Sci.*, **A1**, 1966, **4**, 2607

16   Kruez, J.A., Angelo, R.J. and Barth, W.E., *J.Polym.Sci.*, **A1**, 1967, **5**, 2961

17   Sroog, C.E., *J. Polym. Sci.*, *Macromol. Revs.*, 1976, **11**, 161

18   Karyakin, N.V., Bazhan, N.G., Sapozhnikov, V.N., Shvetsova, K.G., Berestneva, G.L., Lomteva, A.N., Zimini, Yu.B. and Korshak, V.V., *Vysokomol. Soyed.*,1977, **A19**, 1541

19   Sazanov, Y.N., Fedorova, G.N. and Shcherbakova, L.M., *J. Appl. Polym. Sci.*, 1975, **19**, 2335

20   Tsimpris, C.W. and Mayhan, K.G., *J. Polym. Sci.*, *Polym. Phys. Ed.*, 1973, **11**, 1151

21   Hodgkin, J.H., *J. Polym. Sci.*, **A**, 1976, **14**, 409

22   Kilkson, H., *I & EC Fundam.*, 1964, **3**, 281

23   Kilkson, H., *I & EC Fundam.*, 1968, **7**, 354

24   Laius, L.A. and Tsapovetskii, M.I., *Vysokomol. Soyed.*, 1980, **A22**, 226

25   Tsapovetskii, M.I. and Laius, L.A., *Vysokomol. Soyed.*, 1982, **A24**, 979

26   Pal, P.K., Kumar, A. and Gupta, S.K., *Polymer*, 1981, **22**, 1699

27   Misra, M. and Gupta, S.K., *J. Appl. Polym. Sci.*, 1995, **58**, 1877

28   Gupta, S.K., *Numerical Methods for Engineers*, New Age Intl. Publ., New Delhi, 1995

29   Gordon, M., *Proc. Roy. Soc.*, 1962, **A268**, 240

30   Gordon, M., Malcolm, G.N. and Butler, D.S., *Proc. Roy. Soc.*, 1966, **A295**, 29